Chemical Engineering Science Vol. 37, No. 6, pp. 813–844, 1982
Printed in Great Britain.

0009–2509/82/060813–32$16.00/0

REVIEW ARTICLE NUMBER 7

MECHANICALLY AGITATED GAS–LIQUID REACTORS

J. B. JOSHI, A. B. PANDIT and M. M. SHARMA

Department of Chemical Technology, University of Bombay, Matunga, Bombay–400019, India

(*Received* 11 *November* 1981)

Abstract—The hydrodynamic, heat and mass transfer characteristics of mechanically agitated contactors have been critically reviewed. The mixing time (θ_{mix}) can be correlated well by a model based on circulation path and average circulation velocity. Flow patterns in mechanically agitated contactors (single phase) provided with disk turbine, pitched blade turbine and propeller can be characterised. The minimum impeller speed required for the gas induction (N_{cr}) in hollow shaft impellers can be predicted; the minimum impeller speed required for surface aeration (N_s) can also be predicted.

Different strategies of operating mechanically agitated contactors have been examined. The advantages of multistage contactors over single contactors have been stressed.

Recommendations have been made for correlations which can be used for design purpose; lacunae in the available literature have been delineated and recommendations for further work have been made.

CONTENTS

INTRODUCTION

Mechanically agitated contactors are very versatile for conducting a variety of gas–liquid operations, with or without chemical reaction and in the presence or absence of solid particles. The liquid residence time can be varied over a wide range, and semi-batch operation can be adopted for systems which require long residence time. For pure gases the unit can be designed to be "dead-end" type, so that the amount of gas introduced into the reactor balances that consumed. In view of the above and other attributes a variety of reactions, such as, oxidation, hydrogenation, chlorination, carbonation, ozonation, etc. are carried out in mechanically agitated contactors. Even in the field of waste-treatment, very large size contactors are used. In many respects such contactors are considered to be very reliable and scale-up is not considered to be difficult. However, mechanically agitated contactors have many limitations, like high power consumption per unit volume of liquid, gas phase backmixing, sealing of shaft, stability of shaft in tall contactors, etc.

A number of papers and reviews have appeared, covering different aspects of mechanically agitated gas–liquid contactors, in the course of the last decade. However, a coherent theme has not emerged, particularly in aspects dealing with flow patterns, power consumption in the presence of gas, suspension of solid particles, mixing, mass transfer and heat transfer and this review will be concerned with these aspects.

2. HYDRODYNAMICS

2.1 *Flow pattern*

A knowledge of hydrodynamic behaviour is very important for the prediction of the design parameters, such as, heat and mass transfer coefficients and the extent of mixing. It would be highly desirable if we could characterise the velocity field and turbulence in the system. Since disk turbine, pitched blade turbine and propeller are commonly employed in practice, these will be considered for characterising the flow pattern.

2.1.1 *Disk turbine.* In the case of the flat blade disk turbine, which is also known as radial flow impeller, (Fig. 1a) the radial and tangential velocity components are nearly equal in magnitude at the impeller tip but the tangential component decreases more rapidly than the radial velocity component along the radial distance. The average velocity, which is taken as the radial and the tangential component together, is maximum at a certain distance from the impeller tip (Sachs and Rushton[1]). The dimensionless velocity profile, with respect to the impeller tip velocity, has been found to be independent of the impeller speed and has shown slight dependence on the impeller diameter.

The ratio of the radial volumetric flow at the impeller periphery to that of the induced or entrained flow apparently remains constant at 1.9 for all impeller speeds. The pumping capacity of any impeller obeys the following well known correlation:

$$Q = N_Q N D^3 \tag{1}$$

where N_Q is the dimensionless discharge coefficient. The values of N_Q reported by various researchers are given by Uhl and Gray[2] and Bertrand *et al.*[3].

The velocity near the wall is given by the following equation:

$$\bar{v}_{rw} = 0.53\left(\frac{D}{W}\right) N D \left(\frac{D}{T}\right)^{7/6}. \tag{2}$$

The average velocity of the fluid in the bulk can be calculated approximately from the above equation. It will be shown in Section 3, that the circulation model based on the above velocity explains the measured mixing time very well.

The r.m.s. fluctuating velocity has been observed to have two components: (i) periodic component which is

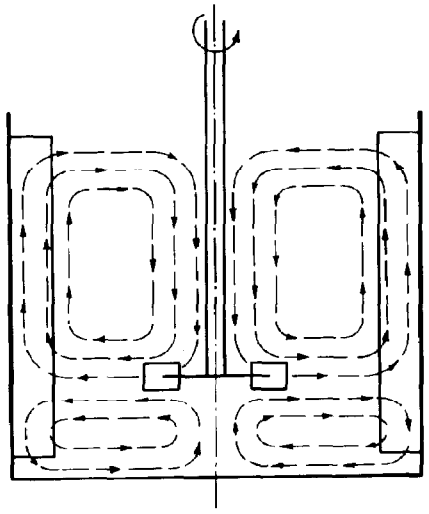

Fig. 1(a). Flow pattern generated by disk turbine or radial flow impeller.

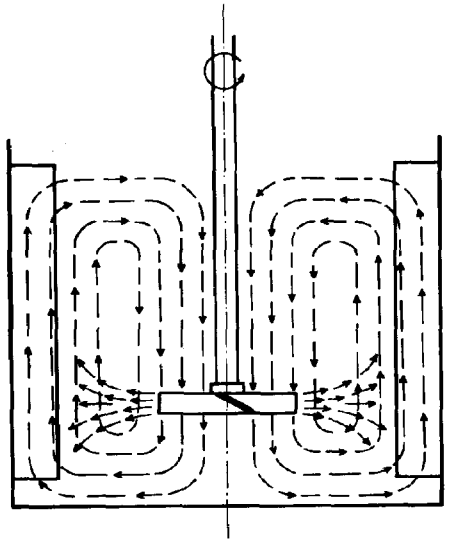

Fig. 1(b). Flow pattern generated by pitched or axial flow turbine.

dominant near the impeller and (ii) the random fluctuating component, which becomes dominant at a certain radial distance from the impeller. The r.m.s. fluctuating velocity in the impeller stream region is about 50–70% of the average fluid velocity, and in the bulk of the tank it is about 5–15% of the average fluid velocity.

The details pertaining to the other type of turbines have been given by Bertrand *et al.*[3].

2.1.2 *Pitched blade turbine.* The information available in the case of pitched blade turbine or popularly known as axial flow turbine is very scanty. The turbine mainly

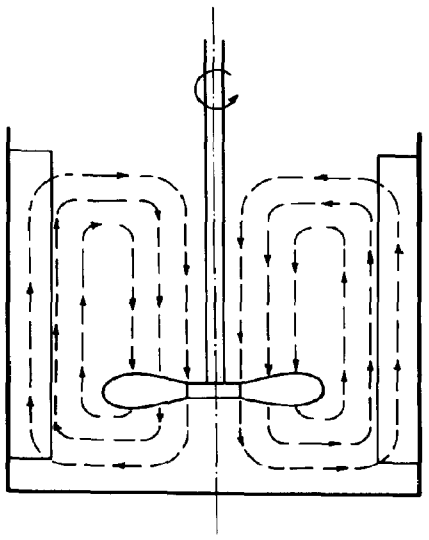

Fig. 1(c). Flow pattern generated by propeller.

produces axial flow with the radial flow proportional to the projected blade width (Fig. 1b). Wolf *et al.*[4] and Levins and Glastonbury[5] have studied the point velocities. Levins and Glastonbury[5] found that the tangential and radial velocities are of comparable magnitude and the vertical velocities are about two times the radial velocity component.

The value of N_Q for pitched blade turbine has been given by Uhl and Gray[2].

The average velocity near the top surface of the fluid in the case of upflow pitched blade turbine and near the bottom of the tank in the case of downflow pitched blade turbine is given by the following equations:

Upflow

$$\bar{v}_{rs} = 0.78\ ND\left(\frac{H - H_i}{D}\right)^{-1} \tag{3}$$

Downflow

$$\bar{v}_{rw} = 0.78ND\left(\frac{H_i}{D}\right)^{-1} \tag{4}$$

2.1.3 *Propeller.* Aiba[6] and Wolf and Manning[4] have made a detailed study of velocity profiles in the case of propellers. Propeller gives mainly axial flow. The flow pattern in the case of propeller is shown in Fig. 1(c).

The position at which the maximum velocity is realised depends on the pitch of the propeller blade. The cross-sectional area of the flowing stream from the impeller does not depend on the impeller speed and is only a function of the vertical distance from the impeller plane. Hence it can be concluded that the extent of entrainment is not a function of the impeller speed, but at higher impeller speeds the discharge velocity only increases, increasing the discharge flow rates. The average values of N_Q have been reported by Marr[7].

The average velocity near the liquid surface or near the bottom of the tank for upflow and downflow system, which are practically the same as the average velocity in the bulk, is given by the following equations:

Upflow

$$\bar{v}_{rs} = 0.65\ ND\left(\frac{H - H_l}{D}\right)^{-1} \tag{5}$$

Downflow

$$\bar{v}_{rw} = 0.65\ ND\left(\frac{H_l}{D}\right)^{-1}. \tag{6}$$

The information regarding turbulence intensities or r.m.s. fluctuating velocities as a function of number of blades, pitch angle, height of the blade in the case of pitched blade turbine and propeller is not available in the published literature and it would be desirable to cover these aspects.

2.1.4 *Flow pattern in the presence of gas.* We have not seen any studies pertaining to the measurement of velocities, pumping capacities and turbulence characteristics of impellers in the presence of gas.

2.1.5 *Recommendation* Equations (2)–(6) are recommended for the calculation of average velocity in the bulk.

2.2 *Power consumption in the presence of gas*

The introduction of gas in mechanically agitated contactors reduces the power consumed by an impeller. This is due to the reduction in the local density of the dispersion as compared to that of pure liquid as suggested by Calderbank[8]. Van't Reit and co-workers[9–11] have suggested that the formation of stable cavity behind the impeller blade reduces the form drag and hence the power consumption. Several investigators have attempted to correlate the reduction in power consumption with parameters, such as, impeller diameter, speed, volumetric gas flow rate and in some cases physical properties of the gas/liquid system. The details pertaining to the range of variables and proposed correlations are given in Table 1.

The gas hold-up in mechanically agitated contactors or the stability of cavity behind the impeller has been found to be, apart from geometric parameters, a function of surface tension, electrolytic nature of solutions, foaming character, etc. Hence phenomenologically the reduction in power consumption should also depend on these characteristics and hence the physical properties of the system. Loiseau *et al.*[12] have found that the foaming character does affect the extent of power reduction. However, these authors could not correlate data for foaming and non-foaming systems by the inclusion of surface tension alone.

Bruijn *et al.*[10], in an attempt to correlate the reduction in the power consumption with the number and the shape of cavities behind the impeller blades, have found that the surface tension does not affect the mechanism of cavity formation and its shape to an appreciable extent. However, liquid viscosity was shown to influence the stability of the cavity but this effect could not be quantified. Calderbank[8] has shown that the gas hold-up varies inversely with the surface tension with a power of 0.55 to 0.65 and this has been supported by Hassan and Robinson[13]. These authors have proposed a correlation which involves surface tension and gas hold-up. Luong and Volesky[14] have also proposed a similar correlation.

Hughmark[15] has made a statistical analysis of all the reported data and found that the coefficient for Weber number (which involves surface tension) was not statistically significant. Further, he found that the use of liquid volume in the place of impeller diameter cube in aeration number and the use of a modified Froude number reduced the average absolute deviation by 50% or more in correlating data of Michel and Miller[16], Pharamond *et al.*[17], Luong and Volesky[14] and Bimbinet *et al.*[18].

The correlation proposed by Hughmark[15] is as follows:

$$\frac{P_g}{P_0} = 0.1\left(\frac{NV}{Q_G}\right)^{1/4}\left(\frac{N^2D^4}{gWV^{2/3}}\right)^{-1/5} \tag{7}$$

This correlation covers the widest range of variables (Table 1) and is dimensionless in character. However it fails at extreme values of gas flow rates.

2.2.1 *Recommendation.* The correlation proposed by Hughmark[15] (eqn 7) is recommended.

2.3 *Suspension of solids*

The suspension of solid particles is of great practical relevance. The solids may act as a catalyst or take part in the reaction. The density of solid particles can vary over a wide range. It is erroneously believed that the introduction of gas improves the quality of suspension (or helps in the suspension of solids). In fact an exactly opposite situation arises and it is found that the introduction of gas results in sedimentation of the particles and at a certain gas flow rate, even complete sedimentation occurs (at a constant impeller speed).

The mechanism of suspension is not clearly understood, though correlations based on different models are available in the literature. The information available can be classified on the basis of the critical or minimum impeller speed required for specified agitator at which complete particle suspension occurs with or without gas.

2.3.1 *Liquid/Solid system.* Zweitering[19], Kolar[20] and Nienow[21] have proposed correlations based on dimensional analysis while Baldi *et al.*[22] have proposed a model based on alternate rising and suspension phenomena arising out of the complex turbulent nature of the flow. They have arrived at a correlation which is similar to that of Zweitering[19]. Narayanan *et al.*[23] have proposed a model based on the minimum pick up velocity, obtained by taking the force balance.

Subba Rao and Taneja[24] have proposed a model, based on the assumption that suspension is only possible when the average liquid circulation velocity in the upward direction is equal or greater than the settling velocity of suspended solids in the population of solid parti-

cles. Einenkel[25] has studied qualitatively the influence of the physical properties and contactor design on the homogeneity of suspension.

It appears that none of the published correlations can predict successfully the effect of impeller position from the tank bottom. Neinow[21] and Zweitering[19] have found that lowering the impeller position reduces the critical impeller speed.

Joosten *et al.*[26] have found that the exponents proposed by Zweitering[19] for parameters like g, D, T, $\Delta\rho$, ρ_T match well even for floating solids.

Among the published correlations Zweittering's correlation covers the widest range and matches well with correlations proposed by Baldi *et al.*[22] or Subba Rao and Teneja[24] is therefore recommended.

2.3.2 *Three phase systems.* Subba Rao and Taneja[24], Short[27], Weildman *et al.*[28] and Chapman *et al.*[29] have studied this system but no correlation has yet been proposed which explains the effect of gas phase satisfactorily.

It is clear from the available data that the critical impeller speed required to suspend the particles increases in the presence of gas under otherwise uniform conditions. This may be due to the reduction in the average liquid circulation velocity because of the reduction in power consumption in the presence of gas.

Subba Rao and Taneja[24] have studied the minimum gas sparging rate required to completely settle the solids and the maximum gas sparging rate which can be used without affecting the solid suspension at critical and two higher impeller speeds. They have proposed the limiting values of these two gas sparging rates as a function of the impeller speed.

For a propeller these limits are:

Complete suspension

$$\frac{Q_G}{(N-N_c)D^3} < 0.5 \times 10^{-2} \tag{8}$$

Partial suspension

$$\frac{Q_G}{(N-N_c)D^3} > 0.5 \times 10^{-2} \text{ up to} < 5 \times 10^{-2} \tag{9}$$

Total sedimentation

$$\frac{Q_G}{ND^3} > 5 \times 10^{-2}. \tag{10}$$

Weildman *et al.*[28] have measured power consumption per unit volume for complete suspension. They found that under aerated conditions power consumption per unit volume increased for maintaining complete suspension. They have made recommendations for the position of an impeller from the bottom for the minimum power consumption. This lies in the range of $0.25 < (H_l/D) < 0.75$ depending upon the concentration of solids. They found that when the gas sparging rate exceeds some critical value the flow from the stirrer declines drastically and escaping gas determines the circulatory liquid flow in the vessel. At a given power per unit volume the flooding point limits the highest dispersable gas flow rate. The lower limiting condition for the complete suspension at a given gas flow rate is governed by the power required for suspension per unit volume. Chapman *et al.*[29] have obtained similar results. They concluded that there is some critical particle density (relative to liquid medium) above which particle suspension governs the power necessary to achieve a well mixed system and below which gas dispersion governs the power requirement. They have reported the values of $\Delta\rho$ as 1500 kg/m^3 when gas introduction causes sedimentation and when $\Delta\rho = 50$ kg/m^3 gas sparging helps the suspension. Details of equipment and variables covered by different authors are given in Table 2.

2.3.3 *Recommendation.* Zweitering[19] and Nienow[21] have suggested the use of larger diameter and lower speed for radial flow impellers and higher speed and smaller diameter for axial flow impellers. In the absence of gas, Zweitering's[19] correlation is recommended. For gas-liquid solid systems the procedure given by Subba Rao and Taneja[24] may be used.

3. MIXING AND R.T.D.

The performance of gas-liquid reactors depend, in addition to the interface mass transfer and intrinsic chemical kinetics, on the extent of mixing in both the phases.

A number of methods of measuring the mixer performance or mixing efficiency have been tried. Different criteria have been used to decide the degree of mixing or homogenity and based on these results, empirical correlations have been proposed for the prediction of dimensionless mixing time "$N\theta$" for different types of agitators and vessel geometries. These correlations together with experimental details are given in Table 3.

3.1 *Effect of design variables on mixing time*

Norwood and Metzner[30], and Biggs[31] have found $N\theta$ to be proportional to $N^{0.34}$ and $N^{0.16}$, respectively. However, most other workers have found $N\theta$ to be essentially constant for a particular impeller.

Impeller diameter

The effect of impeller diameter can be represented by the following equation:

$$N\theta\alpha(T/D)^a \tag{11}$$

where 'a' varies from 2 to 2.57 for the flat blade disk turbines [Khang and Levenspiel[32]; McManamey[33] and "a" is equal to 2 for propellers.

Impeller clearance

Holmes *et al.*[34] have found that lowering of the impeller from the midheight reduced the mixing time while Brennan and Lehrer[35] have found the mixing time to be minimum when the impeller is at midheight. McManamey[33] has shown theoretically that the observation made by Brennan and Lehrer[35] is sound.

Table 1. Survey of variables studied for reduction in power consumption in presence of gas

Reference	System	Agitator type	T	L/T	H/T	H_1/D	V_G m/sec or Q m^3/s	$M=(\frac{P_o^2 ND^3}{Q^{0.56}})$	Constant C in correlation [16]	Exponent over M	Range of physico chemical properties	Correlation proposed
Calderbank [8]	air-water	6 bladed turbine	0.50 0.184	0.33 0.33	1	1	$Q < 8 \times 10^{-5}$ to flooding				ρ_c = 0.79-1.6 x 10^3 kg/m^3 σ = 73.5-21.7 x 10^{-3} N/m μ_c = 0.5-28.0 x 10^{-3} PaS	$\frac{P_g}{P_o} = 1-1.26 \frac{Q_G}{ND^3}$ and $\frac{P_g}{P_o} = 0.62-1.85 \frac{Q_G}{ND^3}$
Nichel and Miller [16]	air-CCl_4	6 bladed turbine	0.165	0.46	0.92	1.33	V_G	150-3500	0.63	0.42	ρ_c = 800 to 1650 kg/m^3 σ = 72-27 x 10^{-3} N/m μ_c = 0.9 to 100 x 10^{-3} PaS	$P_g = C\left(\frac{P_o^2 . ND^3}{Q_G^{0.56}}\right)^{0.45}$
	air-Al_2O_3			0.25	1	1	0.44to10.4	100-31000	1.19	0.42		
	air-Glycerol		0.305	0.33	0.75	0.75	< 0.72	19-38000	0.95	0.43		
Clark and Vermeluen [123]	air-Glycerol	4 blade paddle		0.5			V_G	0.4-1840				$P_g = C\left(\frac{P_o^2 . ND^3}{Q_G^{0.56}}\right)$ exp
	air-Alcohol		0.254		1.6		3.2-22.4		1.20	0.38		
	air-Iso-propanol			0.6				14. -37000				
	air-CCl_4	4 blade paddle	0.254	0.5/0.3	1.6		3.2-22.4	3-15000 0.15-40	2.33	0.33		
		4 blade paddle	0.254	0.5	1.6		3.2-22.4	0.4-3250	1.20	0.38		
Bruijn et al [17]	air-water -water +NaCl -Kero-sene	4 to 18 flat bladed turbines	Square tank 0.5x 0.5x 0.5	0.076	1.0	3.28	Q 0 to flooding				σ = 26 to 76 x 10^{-3} N/m	
Pharamond et al [17]	air-water	6 flat blade turbine	0.29 0.48 1.00	0.33	1.0	0.56	V_G 0.84-05.0 1.5 -06.1 0.88-14.1	100-63000 900-24000 3000-10^7	0.93	0.75	Properties of air-water system	$1-\frac{P_g}{P_o} = 1.6\left(\frac{Q_G}{V}\right) D^{0.63}$ for $(Q_G/V)\, D^{0.63} < 3$
			0.29 0.48 1.00	0.33	1.0	1.0	0.84-05.0 1.5 -06.1 0.88-14.1	100-63000 900-24000 3000-10^7	1.0	0.43		$\frac{P_g}{P_o}$ = 0.8 to 0.55 for $(Q_G/V)\, D^{0.63} > 3$
			0.29 0.48 1.00	0.33	1.0	1.52	0.84-05.0 1.5 -06.1 0.88-14.1	100-63000 900-240000 3000-10^7	1.18	0.48		

Van't Reit et al [11]	air-water	6 bladed convex turbine	0.44	0.4	>1	0.5	V_G < 15	4000-15000	0.80	0.445	Similar to Van't Reit et al.	
		6 bladed concave turbine	0.44	0.4	>1	0.5	< 23.3	3000-10000	1.27	0.44		
		12 blade turbine	0.44	0.4	>1	0.5	< 35	10000-30000	1.16	0.45		
		18 blade turbine	0.44	0.4	>1	0.5	< 41	13000-375000	1.98	0.42		
Hassan and Robinson [13]	air-aqueous solution	4 to 6 blade paddle/ turbine	0.152 0.291	1/3 / 2/3	1	1	V_G 03.5-68 5 -22.1				ρ =1000 to 1100 kg/m^3 σ =(74-44)x10^{-3} N/m μ_e=(0.8-3.0)x10^{-2} PaS	$\frac{P_g}{P_o} = C(\frac{N^2D^3\rho_L}{\sigma})^m (\frac{Q_G}{ND^3})^n (\frac{\rho_L}{\rho_G})$ n=0.38 m=-0.22 4b paddle m=-0.25 6b turbine
Loiseau et al. [12]	air-Glycol air-ethanol air-water +HCl+CuCl	6 flat blade Rushton type	0.225 0.15	0.33	1.0	1.0	V_G 0.75-85	1 - 200000	0.83	0.45	Nonfoaming ρ =0.803 to 1.278 x10^3 kg/m^3 σ =61-2[illegible]x10^{-3} N/m μ =(1-48.5)x10^{-3} PaS	$P_g = C(\frac{P_o^2 ND^3}{Q_G^{0.56}})^{exp}$
	air-Aq.Sod. sulphite air-Acetic Acid+Propanoldehyde								0.69 1.88	0.45 0.31	Foaming ρ =1085 to 1158 kg/m^3 σ =56 to 54x10^{-3} N/m μ =(1.50 to 5.40) x10^{-3} PaS	If M < 2 x 10^3 M > 2 x 10^3
Luong and Volesky [14]	air-Glycol air-CMC solu.	6 flat bladed turbine	0.22	0.33	1.0	1.0					ρ =983 to 1100 kg/m^3 σ =72 to 55x10^{-3} N/m μ =(0.85 to 3.0) x10^{-3} PaS	$\frac{P_g}{P_o} = C(\frac{N^2D^3\rho_L}{\sigma})^m (\frac{Q_G}{ND^3})^n$ m= -0.18 (a) For Newtonian m= -0.194 (b) For Non Newtonian n= -0.38, C= 0.497 (a), C= 0.514 (b)
Yung, Wong and Chang [124]	air-Tap water air-Glycol air-Acetone	6 bladed turbine and 4 bladed paddle	0.4 flat 0.4 hemi	0.225 0.325 0.45	1.0 1.0 1.0	1.0 1.0 1.0	Q 1.22x10^{-4} 27.2 x10^{-4}	N r/s 3.33-23.3	0.812	0.45	ρ =960 to 1047 kg/m^3 σ =(58.29-72.74) x10^{-3} N/m μ =(0.80-2.10)x 10^{-3} PaS	$P_g = C(\frac{P_o^2 ND^3}{Q_G^{0.56}})^{exp}$
	air-NaCl solm. air-Na_2SO_4 soln.		0.4 flat 0.4 hemi	0.225 0.325	1.0 1.0	1.0 1.0	Q 1.22x10^{-4} 27.2x10^{-4}	N r/s 3.33-23.3	0.889	0.45		

Table 2. Suspension of solids in mechanically agitated gas–liquid contactor

Sr. No.	Author	System	Impeller type	T,(m)	D,(m)	H,(m)	H_1,(m)	Solid size μ	Solid density kg/m³	Gas flow rate cm³/sec
1.	Gubbarao and Taneja [24]	air-water-river sand Badarpur sand glass balls	Propeller	0.164	0.0508	0.164		63-75 106-125 152-163 500-699 3070	2704.9 2704.9 2704.9 2666.1 3009.7	(0 to 100) x 10^{-6}
2.	Short [27]	air-water-Lucite pellets (p methyl-methacrylate)	4 bladed 45° pitched blade turbine	0.91	0.43 0.56	0.91 to 1.52 elliptical bottom				0 to 0.047
3.	Wieldmann et al [28]	air-water-glass beads	Rushton turbine, propeller	0.2	0.066	0.2	0.017 to 0.05	298 430	2500	1.57×10^{-5} 3.14×10^{-3}
4.	Chapman et al [29]	air-water-polystyrene glass powder ballotini	Rushton turbine, propeller	0.56	0.14, 0.185, 0.29	0.54	0.14	250-355 250-355 180-250	1050 2200 2480	(0.57 to 2.9) x 10^{-3}

Impeller blade width

The effect of blade width on θ is dependent on the impeller speed, position and geometry of the vessel (Brennan and Lehrer[35]). McManamey[33] tried to correlate the effect of blade width with the power requirement but no conclusive effect could be found. The circulation model discussed by us in this review based on the average liquid circulation velocity explains the effect of (W/D) successfully $[0.125 < (W/D) < 0.2]$. (see section 3.2.1). Data outside this range are not available in the literature to check the soundness of the model in explaining the effect of (W/D).

3.2 *Theoretical analysis*

Rao *et al.*[36], Goldstein[37], Brennan and Lehrer[35], and Sasakura *et al.*[38] have analysed the problem of mixing on the basis of complex models containing some combination of plug flow and completely backmixed units and superimposed by cross flow and by-pass. We will, however, discuss a method of calculating mixing time on the basis of liquid circulation velocity. Initially the method will be applied to the case where gas is absent. Subsequently the method will be extended to explain the effect of the presence of gas on the mixing time.

Joshi[39] has calculated the average liquid circulation velocity on the basis of mixing time and the maximum length of circulation loop. The circulation velocity obtained in this manner agrees well with the experimentally measured values and hence an exactly reverse procedure can, in practice, be followed to calculate the mixing time.

McManamey[33] has explained successfully the functional dependence of mixing time on the impeller speed, (D/T), and impeller height from the bottom and to some extent the effect of blade width on mixing time. The use of average liquid circulation velocity and maximum loop length were used to explain the effect of various parameters.

The circulation model which will be used by us to predict the mixing time has the following features:

(1) Mixing time is directly proportional to the longest loop length which depends on the type of the impeller and the position. The longest loops are shown in Fig. 2, 3 and 4 for various impellers.

(2) Mixing time is inversely proportional to the average circulation velocity near the wall (in the case of flat blade turbine) or near the surface (upflow propeller) or in other words where the longest circulation loop exists.

(3) Mixing time θ is taken equal to 5 times the circulation time. This assumption is based on the studies of Prochazka *et al.*[40] and Holmes *et al.*[34], which indicate that after 5 circulations 99% of the mixing is complete.

(4) Flow is fully turbulent and the dimensionless velocity (v/ND) is independent of the impeller speed.

3.2.1 *Flat blade turbine.* Van der Molen and Van Maanen[41] have given an equation for the average circulation velocity for standard flat blade turbine. This equation can be written in the following form:

$$\bar{v}_{rw} = 0.53\left(\frac{D}{W}\right)ND\left(\frac{D}{T}\right)^{7/6} \tag{12}$$

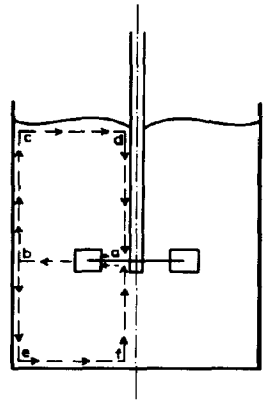

Fig. 2. Length of longest circulation path in case of disk turbine.

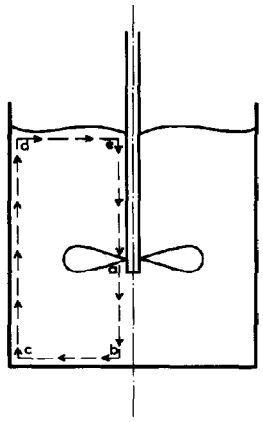

Fig. 3. length of longest circulation path in case of propeller.

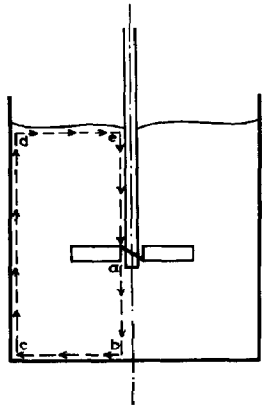

Fig. 4. Length of longest circulation path in case of pitched blade turbine.

where $\bar{v}_m$ is average liquid velocity near the wall including the entrainment effect.

From the flow pattern of the turbine the longest loop is either "abcda" or "abefa" (Fig. 2) depending upon the position of the impeller. Hence in general the longest loop length is written as $(aH + T)$ where a is equal to one when impeller is situated centrally or equal to 1.33 if H_i is equal to $H/3$ and so on. Hence,

$$\text{Circulation time, } t_c = \frac{\text{Length of the longest loop}}{\text{Average circulation velocity}}$$

Thus for standard flat blade turbine, where $N_p = 5$,

$$t_c = \frac{(aH + T)}{0.53(D/W)ND(D/T)^{7/6}} \tag{13}$$

and

$$\theta = 5t_c$$

$$\therefore \quad N\theta = 9.43\left[\frac{aH + T}{T}\right](T/D)^{13/6}(W/D). \tag{14}$$

3.2.2 *Propeller and pitched blade turbine.* In the case of propeller and pitched blade turbine, the velocity profile can be written as:

For downflow

$$\bar{v} = cND\left(\frac{H_i}{D}\right)^{-1} \tag{15}$$

For upflow

$$\bar{v} = cND\left(\frac{H - H_i}{D}\right)^{-1} \tag{16}$$

where the constant c is determined by comparing the average velocity near the impeller which is calculated as:

$$\bar{v} = \frac{N_Q \cdot ND^3}{\frac{\pi D^2}{4}}. \tag{17}$$

$N_Q = 0.65$ in the case of propeller (Section 2.1) and $N_Q = 0.78$ in the case of pitched blade turbine (Section 2.1).

Now in the case of propeller and pitched blade turbine the flow pattern is essentially the same and the longest loop is "abcdea" (Fig. 3 and Fig. 4).

Thus we get the following equations for propeller:

Downflow

$$N\theta = 6.0\left(\frac{2H}{D} + \frac{T}{D}\right)\left(\frac{H_i}{D}\right) \tag{18}$$

Upflow

$$N\theta = 6.0\left(\frac{2H}{D} + \frac{T}{D}\right)\left(\frac{H - H_i}{D}\right). \tag{19}$$

And for pitched blade turbine:

Downflow

$$N\theta = 5.0\left(\frac{2H}{D} + \frac{T}{D}\right)\left(\frac{H_i}{D}\right) \tag{20}$$

Upflow

$$N\theta = 5.0\left(\frac{2H}{D} + \frac{T}{D}\right)\left(\frac{H - H_i}{D}\right). \tag{21}$$

Data on the flat blade turbines are compared with the theoretical prediction of the circulation model, in Fig. 5. We can conclude that the circulation model satisfactorily predicts $N\theta$ values which are constant for a particular geometry.

It appears that at higher (D/T) ratios mixing time predicted by the circulation model matches very well than at lower (D/T) ratios. As the circulation model is based on pumping capacity and the circulatory flow, larger (D/T) ratio encourages flow of liquid rather than

Table 3. Survey of correlation proposed for measurement of mixing time

Reference	Method	Criteria	Impeller type	Vessel diameter T (m)	Impeller diameter D (m)	Correlation
Fox and Gex [125]			Propellers ubaffled tank	0.15 to 4.20	0.05 to 1.38	$\frac{\theta (ND)^{2/3} g^{1/6}}{H^{1/2} T} \sim (Re)^{-1/6}$
Kramers et al. [126]	Conductivity measurement	Time reqd. to reach 0.1 % of the final concn.	Propellers, turbines baffled tank	0.32, 0.64	Propeller: 0.08, 0.16 Turbine : 0.16	$N\theta \sim$ constant
Van de Vusse [127]	Refractive index measurement	Time from starting of agitator to disappearance of last streak	Paddles, turbines unbaffled propellers	0.135, 0.49	Propeller: 0.076, 0.16 Turbine :	$N\theta \sim (N^2 D)^{-1/3}$ $N\theta \sim N^{1/2} D^{1/4}$
Norwood et al. [30]	Decolourisation Methyl red.	Time for decolouration of methyl red	Turbines baffled	0.14 to 0.40	0.10, 0.07	$\frac{\theta (ND)^{2/3} g^{1/6}}{H^{1/2} T} \sim$ constant
Biggs [31]	Conductivity measurement	Time reqd. to reach 5 % of well mix concn.	Propellers, paddles turbine, baffled	0.25	Propeller: 0.077 Paddle : 0.11 Turbine : 0.06, 0.10	$\frac{\theta N^{2/3} D^{4/6} g^{1/6}}{H^{1/3} T^{3/2}} \sim$ constant
Holmes et al. [34]	Conductivity measurement	Circulation time equal to time delay in concentration peaks and 5 circulation time equal to mixing time	Turbines baffled tank	0.22, 0.60, 1.00	0.039 to 0.44	$N\theta (D/T)^2 \sim$ constant
Prochazka and Landau [40]	Conductivity measurement	Time from addition of pulse to a fractional completion of change in conductivity	Propellers, baffled, paddles, baffled turbines baffled	0.35	Propeller: 0.05 paddle : 0.056 Turbine : 0.056	$N\theta (D/T)^{2.05} \sim$ constant $N\theta (D/T)^{2.20} \sim$ constant $N\theta (D/T)^{2.57} \sim$ constant

Wesselingh [128]	Conductivity measurement	Homogeneous conductance Mixing of two immiscible liquids	Side entering propeller			$N\theta = 1500(T/L)^{1.3}\left(\frac{H}{T}\right)^{2.4}(H_1/H)\left(\frac{F_{rc}}{F_r}\right)^{1.5} + 180\,(T/D)^{1.3}\,(H/T)^{0.8}$ where, H_1 = Height of heavier liquid.
Mersmann et al. [129]			Data of Zlokarnik (1967), Kramers (1953) Vande Vusse (1959) Biggs (1963) Gramlick (1973)			$N\theta = 6.7\,(L/T)^{-5/3}\,(N_p)^{-1/3}$
Khang and Levenspiel [32]	Conductivity measurement	Upto desired amplitude of conductivity v/s time for pulse response	Turbine For propeller	0.559, 1.219	Propeller, Turbine 0.114 to 0.366	$\left(\frac{N}{K}\right)\left(\frac{D}{T}\right)^{2.3} = \frac{P\,g_c}{\rho N^3 D^5} \simeq 0.5$ for $Re > 10^4$ $\left(\frac{N}{K}\right)\left(\frac{D}{T}\right)^{2.0} = 1.5\,\frac{P\,g_c}{\rho N^3 D^5} \simeq 0.9$ for $Re > 10^4$ $\frac{N}{K}$ = mixing rate number N_{mix} K = Decay rate constant
Burghargt and Lipowska [130]						$N\theta = 2428.2\,(Re_p)^{-1.215}\,(L/T)^{0.088}$
Sasakura et al. [36]	Conductivity measurement	Disappearance of conductivity peak	Paddles fully baffled	0.30		$\left(\frac{1}{(N\theta)^2} - \frac{0.518}{(Nt_c)^2}\right)^{1/2} = K\left(\frac{T}{D}\right)^{3/2}\left(\frac{1}{Nt_c \cdot N_p}\right)^{1/2}$
			In the presence of gas			
Pača et al. [79]	Conductivity measurement	-	3 Turbines	0.508 (multistage)	0.17	--
Einsele et al [43]	pH meter	Constant reading	Turbine	0.285, 0.756	Not stated	$\theta_a / \theta_{mix} = 1 + 7.5(\mu)^{0.27}\,(\epsilon_G)$ $\theta_a = (\theta_{mix})$ in presence of gas.

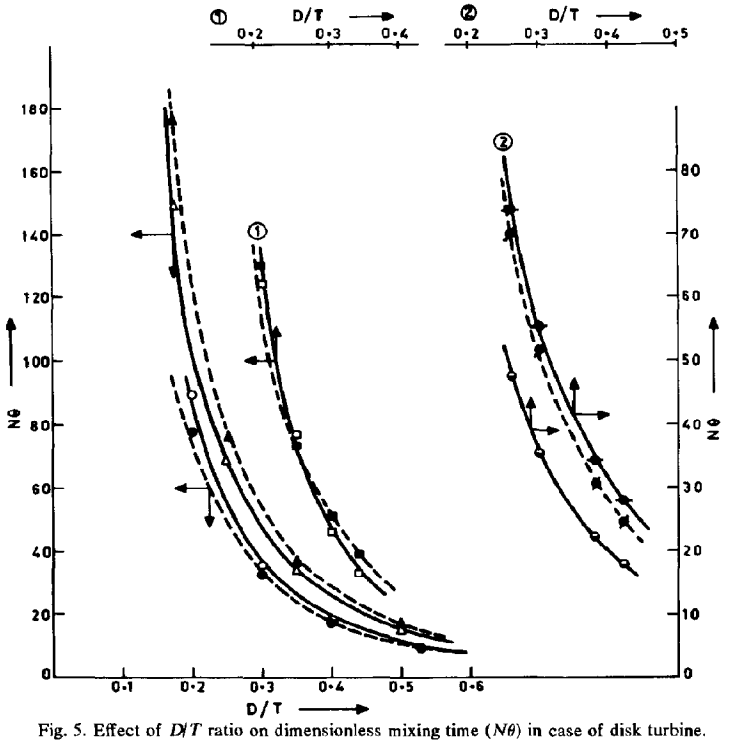

Fig. 5. Effect of D/T ratio on dimensionless mixing time ($N\theta$) in case of disk turbine.

Symbol	Tm	W/D	Author
(a) ● ●	0.145—0.395	0.2	Norwood and Metzner[30]
			Predicted by eqn (14)
(b) ◒ ●	0.245	0.2	Biggs[31]
			Predicted by eqn (14)
(c) △ ▲	0.22,0.6,1.0	0.2	Holmes *et al.*[34]
			Predicted by eqn (14)
(d) □ ■	0.550	0.2	Prochazka and Landau[40]
			Predicted by eqn (14)
(e) ○ ●	0.144,0.211, 0.314	0.125	Chemineer Inc. Handbook[125]
			Predicted by eqn (14)

turbulence which is the main form of energy dissipation in the case of smaller impellers (Davies[42]). Thus the results of experiments and theory match well for larger impellers.

Similarly larger (W/D) ratio also reduces the mixing time due to the increase in the pumping capacity.

In the case of propeller data from Uhl and Gray[2] were tested. They match satisfactorily with the prediction of the circulation model. The sudden drop in $N\theta$ reported in their data can be explained with the assumption of smaller loops operating simultaneously rather than a single long loop operating.* A comparison between the prediction of the circulation model and observed values is shown in Table 4.*

3.3 *Mixing time in the presence of gas*

The average circulation velocity, including the entrainment effect as explained by Vander Molen and Van Maanen[41], can also be written in the form given in eqn (12).

$$\text{or} \qquad \bar{v}_{rw} = 0.309 \times N_p^{1/3} \left(\frac{D}{W}\right) ND \left(\frac{D}{T}\right)^{7/6}. \tag{22}$$

Now in the presence of gas the above equation can be written as:

$$\bar{v}_{rw}' = 0.309 \times \left(\frac{P_g}{\rho_L N^3 D^5}\right)^{1/3} \left(\frac{D}{W}\right) ND \left(\frac{D}{T}\right)^{7/6}. \tag{23}$$

We now make use of the correlation proposed by Hughmark[15] for P_g and we get:

$$\bar{v}_{rw} = 0.309(0.1N_p)^{1/3} \cdot \left(\frac{Q_g}{NV}\right)^{-1/12} \left(\frac{N^2D^2}{gWV^{2/3}}\right)^{-1/15} \times \left(\frac{D}{W}\right) ND \left(\frac{D}{T}\right)^{7/6}. \tag{24}$$

Table 4. Comparison between $N\theta_{predicted}$ and $N\theta_{expt}$ for propeller

S.No.	Diameter D (m)	H (m)	$(N\theta)_{exptl}$	$(N\theta)_{predicted}$	*
1	0.0762	0.147	37.0	60.25	
2	"	0.196	48.0	70.35	
3	"	0.244	35.0	80.4	55.78
4	"	0.292	56.0	90.25	65.88
5	"	0.342	75.0	100.5	75.9
6	0.1016	0.147	21.2	33.9	
7	"	0.196	28.0	39.6	
8	"	0.244	23.0	45.2	31.38
9	"	0.292	37.0	50.75	36.91
10	"	0.342	50.0	56.55	42.72
11	0.114	0.147	18.2	26.75	
12	"	0.196	21.0	31.2	
13	"	0.244	29.5	35.7	
14	"	0.292	36.5	40.1	
15	"	0.342	41.2	44.0	
16	0.127	0.147	16.5	21.7	
17	"	0.196	20.7	25.3	
18	"	0.244	26.0	28.15	
19	"	0.292	29.5	32.45	
20	"	0.342	35.2	36.21	

The use of this circulation velocity and the longest loop length for the flat blade turbine gives:

$$N\theta = 20.41\left[\frac{H}{T}+1\right] \times \left(\frac{T}{D}\right)^{13/6}\left(\frac{W}{D}\right)\left(\frac{Q_g}{NV}\right)^{1/12}\left(\frac{N^2D^4}{gWV^{2/3}}\right)^{1/15}. \quad (25)$$

A comparison between the predicted and the experimental (Einsele and Flnn[43]) values of $N\theta$ is shown in Fig. 6. As can be seen from this figure, the predicted mixing time by the circulation model matches with the experimental values within 30%. The values of $N\theta$, predicted by this model are always higher. Additional data are required to throw further light, but the analysis presented here appears to lead to reasonably accurate values of $N\theta$.

3.4 *Mixing in gas phase*

Westerterp *et al.*[44] have measured the thermal conductivity of the exit gases. They have observed the existence of a critical impeller speed (N_0) below which the impeller speed had no influence on the gas phase hold-up, but above this speed the gas hold-up was dependent only on the impeller speed and was independent of the gas flow rate. The absolute spread in R.T.D. was found to increase as a function of the gas phase hold-up or impeller speed. Hanhart *et al.*[45] have found that, depending upon the impeller diameter and the clearance from the bottom, the gas phase R.T.D. was equivalent to a single ideal CSTR or two ideal CSTR's in series; or in between the two. Gal-Or and Resnick[46] have observed similar results in terms of broadening of R.T.D. as a function of the impeller speed. They had also used the thermal conductivity measurement technique with helium as a tracer. But in contrast to Hanhart *et al.*[45] they found the narrowing of R.T.D. as a function of the impeller speed. Gal-Or and Resnick[46] could fit the experimental gas phase R.T.D. with the theoretically calculated R.T.D. of two perfectly mixed stirred cells in series and 15% of the gas introduced flowing in a plug flow manner.

Van't Reit *et al.*[11] have found that the maximum interaction between the bubbles is near the impeller. They have also found that with an increase in the number of blades, the coalescence of gas bubbles with stable cavities behind the impeller blade increases, resulting in an increase in the gas phase mixing rate. Mehta and Sharma[47] varied the outlet partial pressure of the solute gas while measuring the effective interfacial area (a) by chemical methods. It was found that, under otherwise identical conditions, the values of a were found to be practically constant when based on the completely backmixed behaviour of the solute gas. Juvekar[48] has followed a similar procedure and found that the gas phase moves in a plug flow manner when solid particles (fine calcium carbonate particles) are present in the liquid phase.

Unfortunately very limited data on the gas phase backmixing are available in the published literature. Further studies should be carried out in contactors larger than 50 cm i.d. and should include the effect of N, D, T, type of the impeller and the properties of gas–liquid system on the gas phase backmixing. The physical properties of G/L system influence the values of the functional gas hold-up which in turn affects the circulation velocity and mixing time.

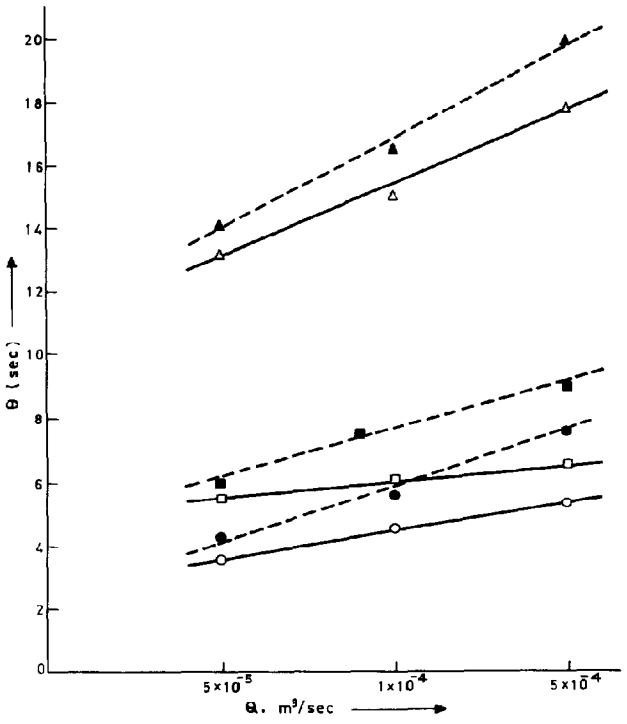

Fig. 6. Effect of presence of gas on mixing time (θ). Einsele and Flnn[43], $T = 0.285$, $D = 0.095$, System air–water.

	Symbol	Impeller speed (r/s)
(a)	△	3.33
	▲	Predicted by eqn (25)
(b)	□	8.33
	■	Predicted by eqn (25)
(c)	○	13.33
	●	Predicted by eqn (25)

3.5 *Recommendation*

For the calculation of mixing time in absence of gas equations (14),(18–21) are recommended for specified impellers. At present there is very limited information to recommend any correlation for the gas phase mixing in *G/L* and *G/L/S* systems. However, it appears that above the critical speed of impeller the gas phase is closer to being backmixed in *G/L* systems.

4. MASS TRANSFER

In most industrial applications mass transfer is accompanied by chemical reaction. It is necessary to know the value of effective interfacial area and the liquid side mass transfer coefficient.

4.1.1 *Effective interfacial area.* For the measurement of the effective interfacial area the following methods have been used: (i) physical: Photography, light reflection and light scattering; (ii) Chemical.

Towell *et al.*[49], Burges and Calderbank[50] and Schumpe and Deckwer[51] have shown that the results obtained from the photographic technique are subject to serious uncertainties depending upon the properties of the system and the manner of taking the photographs. Calderbank *et al.*[52] have suggested the light reflection technique. However this method measures the interfacial area at the column wall.

The light scattering method was also introduced by Calderbank[8]. This method can conveniently be used when the product al (Effective interfacial area x·light path length) is less than 20 (Lokett and Safekourdi[53]). Above this value, multiple scattering increasingly contributes to the overall error. Landau *et al.*[54], Weinstein and Treybal[55] and McLaughlin and Rushton[56] have suggested methods to reduce this error. The light scattering method is laborious if the mechanically agitated contactor is relatively of larger size.

Chemical methods

Sharma and Danckwerts[57] have discussed in detail the chemical methods of measuring a. Over the years, several systems have been reported in the published literature for the measurement of a by chemical

methods. Danckwerts and Sharma[58], Jhaveri and Sharma[59] and Sridharan and Sharma[60] have successfully used these methods.

Recently Schumpe and Deckwer[51] and Midoux *et al.*[61] have discussed the limitations of chemical methods. The major drawback associated with this method is the uncertainty regarding the backmixing in the gas phase. This limitation can be overcome by using lean O_2–sodium dithionite system. In this case conversion with respect to gas phase is relatively small and the intrinsic reaction is zero order in O_2 and therefore the rate of absorption varies as the square root of p_{O_2}. Sulphite (sodium and potassium) oxidation is also used for the measurement of a. The kinetics of the reaction and the various factors affecting the kinetics has been reviewed by Linek and Vacek[62].

4.1.2 *Liquid side mass transfer coefficient* ($k_L a$). The methods for the measurement of $k_L a$ include;

(i) Physical: Absorption or desorption of a gas under unsteady state conditions.

(ii) Chemical: Van't Reit[63] has reviewed the method in detail. The effect of the dynamics of the concentration measuring instrument and the errors associated with the dynamic behaviour of the gas hold-up have been discussed. Recently, Keitel and Onken[64] have discussed the sources of inaccuracies in the measurement of $k_L a$. The errors associated or originated mainly from the assumptions regarding the degree of mixing in both the phases and from the experimental uncertainties.

The absorption of lean carbon dioxide in carbonate buffer solutions (sodium carbonate–bicarbonate) and the absorption of oxygen in acidic cuprous chloride solutions are some of these systems which can be employed. Sharma and Danckwerts[57] and Sharma and Mashelkar[65] have reported the pertinent details. Sridharan and Sharma[60] have used the absorption of carbon monoxide or propylene in cuprous ammonium complex solutions. In this case absorption is accompanied by an instantaneous chemical reaction.

4.1.3 *Simultaneous measurement of a and $k_L a$.* Usually different systems are used for the measurement of a and $k_L a$ and it is likely that the hydrodynamic behaviour is different for the different systems. Juvekar and Sharma[66] have sucessfully employed the oxygen–sodium dithionite system for this purpose. By manipulating the oxygen partial pressure and the concentration of sodium dithionite the conditions for the measurement of a and $k_L a$ can conveniently be selected. A number of measurements have been reported in the literature where $k_L a$ are measured simultaneously by desorbing a physically dissolved gas where absorption of a gas is accompanied by a fast pseudo m^{th} order reaction.

4.1.4 *Gas side mass transfer coefficient.* There are no data available in the published literature on the gas side mass transfer coefficient. The principal difficulty lies in the fact that the conversions with respect to solute gases are very high in gas-film controlled operations and a precise knowledge of the degree of backmixing in the gas phase is necessary for the evaluation of $k_G a$.

4.2 *Correlation of data*

Effective interfacial area is given by the following equation:

$$a = \frac{6\epsilon_G}{d_B} \tag{26}$$

where ϵ_G and d_B are average values of fractional gas hold-up and the bubble diameter, respectively. It is known that the variation of both ϵ_G and d_B is very wide in the vessel and only the average values of a are available from the experimental determinations. The details pertaining to the experiments are summarised in Table 5.

A plot of a vs impeller speed is shown in Fig. 7. (Mehta and Sharma[47]). It can be seen from Fig. 7 that, at a particular value of the superficial gas velocity, the value of a is practically constant irrespective of the impeller speed. At a certain impeller speed, a starts increasing with N and at relatively high impeller speeds a varies linearly with N. An extrapolation of the linear part of the plot gives the value of N_0, the critical impeller speed, Westerterp *et al.*[44] and Mehta and Sharma[47] and Juvekar[48] have shown that, above the value of N_0, a is practically independent of the superficial gas velocity. Westerterp *et al.*[44] have suggested the following equation for the critical impeller speed (N_0):

$$\frac{N_0 D}{\left(\frac{\sigma g}{\rho}\right)^{1/4}} = A + B\frac{T}{D} \tag{27}$$

where, the term $(\sigma g/\rho)^{1/4}$ has the significance of the rise velocity of the bubble. In the absence of an impeller, the fractional gas hold-up depends upon the superficial gas velocity. In the presence of an impeller, because of the intense circulatory liquid flow pattern, the bubbles are returned to the impeller and the gas hold-up is higher than that in the absence of the impeller. With an increase in the impeller speed the contribution of the impeller in deciding the gas hold-up and the bubble diameter increases. As an approximate estimate, the relative contribution of the impeller and sparging towards the gas dispersion is determined from the respective energy input rates. The other way of estimation is the intensity of liquid flow pattern generated by individual actions. For instance, in the case of the standard six bladed disk turbine, when centrally located, the liquid circulation velocity is given by the following equation (Joshi *et al.*[39]).

$$V_c = 1.86\frac{ND^2}{T} \tag{28}$$

In the case of sparging alone, the average liquid circulation velocity is:

$$V_c = 1.31\{gT(V_G - \epsilon_G V_{b\infty})\}^{1/3}. \tag{29}$$

For instance in the case of ($T = 0.5$ m, $D/T = 1/3$, $V_G =$ 30 mm/sec and $P/V = 0.1$ kW/m^3) the values of circulation velocity in the case of mechanically agitated contactors and bubble columns were found to be 0.16

Table 5. Experimental details for the determination of a and k_La

Sr. No.	Reference	System	column diameter T (m)	D/T	Impeller Speed N (r/s)	Method of measurement	Correlation or correlating parameters
1.	Calderbank [8]	air-water	0.2, 0.5	0.33	3-50	Photographic	$a = \left[\frac{1.44(\frac{P_G}{V})^{0.4}\rho_L^{0.2}}{\sigma^{0.6}}\right] \times (V_G/V_{b\infty})^{0.5}$
2.	Westerterp et al [44]	1 lean O_2-sodium sulphite	0.14, 0.15, 0.19, 0.6, 0.9	0.2 to 0.7	1.67 to 60	Chemical	$a = \frac{(7.5\pm1.2)\times10^{-5}}{\sqrt{KD/\epsilon}\, H_e \times D\sqrt{\rho_L T/\sigma}} (\frac{N-N_o}{H})$
3.	Mehta and Sharma [47]	1 lean CO_2-NaOH or KOH 1 lean CO_2-aqueous sons. of alkanolamines 1 lean O_2-CuOl 2 lean CO_2-Na_2CO_3+$NaHCO_3$	0.125, 0.2, 0.4, 0.7	0.29 to 0.52	4-32	Chemical	$ND/\sqrt{T}$
4.	Prasher and Wills [131]	lean CO_2-water lean CO_2-NaOH	0.29	0.3	1-6	Physical and chemical	$k_L = 0.592\, D_A^{1/2} (\frac{P_G \rho_L}{\rho_L V \mu})^{1/2}$
5.	Miller [67]	lean CO_2-water	0.45, 0.31, 0.67	0.66*	0.42-7	Physical desorption	$a = \frac{1.44(P_G/V)^{0.4}\rho_L^{0.2}}{\sigma^{0.6}} \times \{V_G/(V_G+V_{b\infty})\}^{0.5}$
6.	Juvekar [48]	lean O_2-sodium dithionite lean CO_2-Na_2CO_3+ $NaHCO_3$	0.75, 1 0.75, 1	0.3 to 0.7	2.0 to 6.33	Chemical	$\frac{ND}{\sqrt{T}}$, $\frac{(N-N_o)\,L}{\sqrt{T}}$ $(\frac{P_G}{V})^{0.4}$, $(\frac{P_G}{V})^{0.4}\epsilon_G^{0.5}$
7.	Hassan and Robinson [132,133]	air-water+electrolyte	0.15	0.33	12.2 to 31.7	Chemical[1] Physical desorption	
8.	Sridhar and Potter** [134]	O_2-Cyclohaxane	0.13	0.35	17.5 to 25.0	Resistivity probes and γ ray transmission	$a = 1.44(P_G/V)^{0.4}(\rho_L^{0.2}/\sigma^{0.16})(\frac{V_G}{V_{b\infty}})^{0.5}(\frac{\rho_T}{\rho_G})(\frac{\rho_G}{\rho_{air}})^{0.16}$
9.	Lopes de Figueredo and Calderbank [68]	air-water	0.38, 0.91	0.3, 0.33	4.16 to 8.33	[1]Light transmission Physical absorption	$a = 593(P_G/V)^{1/4} V_G^{3/4}$ $k_La = \frac{1\times10^{-3}}{V_L} P_G^{0.58} V_G^{3/4} T$
10.	Chandrashekharan and Calderbank [69]	air-water	1.22	0.3	4.4	Physical absorption	$k_La = \frac{0.0248}{T^4}(\frac{P_G}{V})^{0.55} \times \rho_G^{0.551/\sqrt{T}}$

* Four bladed impeller. In all the other cases six bladed disk turbine was employed.
** The procedure for the calculation of total power input is given.

and 0.49 m/sec, respectively. By contrast for the case of ($T = 1$ m, $D/T = 1/3$, $V_G = 5$ mm/sec and $P/V = 10$ kW/m^3) the corresponding values are 1.49 and 0.3, m/s, respectively).

Calderbank[8], Miller[67], Lopes de Figueiredo and Claderbank[68] and Calderbank and Chandrashekhar[69] have shown that the values of a and k_La vary as V_G^x where x varies in the range of 0.5 to 0.75. The above discrepancy regarding the effect of V_G may be because of the following reasons:

(i) Westerterp *et al.*[44] and Mehta and Sharma[47] have used non-coalescing systems (aqueous solutions containing an electrolyte) whereas Calderbank *et al.* have used coalescing system (air-water). The average bubble diameter in the former case is about 3 to 5 times smaller than that in air-water system. Therefore, the rise velo-

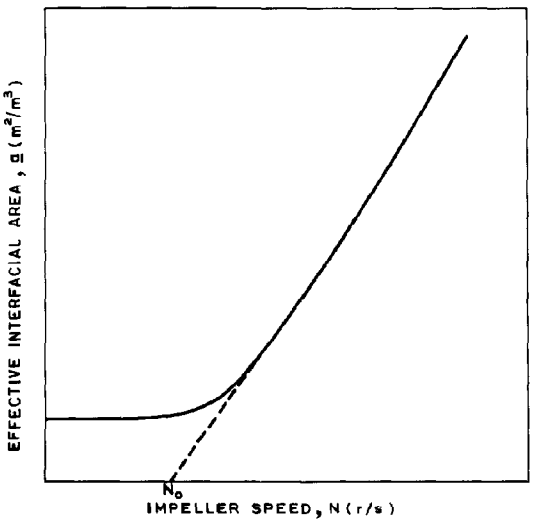

Fig. 7. Dependence of effective interfacial area (a) on impeller speed.

city of a bubble in non-coalescing system will be about 2 times lower than that in the coalescing system. This difference is not observed from the term $(\sigma g/\rho)^{1/4}$ for the rise velocity of a bubble in eqn (26). However, it is expected that the value of N_0 in coalescing system should probably be much higher than in the noncoalescing system.

(ii) For large diameter vessels, it is likely that the impeller speed will be relatively high in order to induce the backflow of bubbles. Consequently, the critical impeller speed probably increases with the vessel diameter.

Above the critical impeller speed the values of a and k_La have been correlated in different ways. The various correlations together with the equipment details are summarised in Table 6. The earlier correlations reported by Calderbank[8] indicate that a and k_La vary as $(P_G/V)^{0.4}$ and k_L is practically independent of P/V. The recent work of Calderbank *et al.*[68,69] indicates that the values of a and k_La vary as $(P/V)^{0.25}$ and $(P/V)^{0.55}$ respectively. Further V_G had substantial influence on a and k_La even above the critical impeller speed. It may be emphasized that the system air–water was common in all the cases.

Mehta and Sharma[47] have analysed a and k_La data from 0.125, 0.2, 0.4 and 0.7 m i.d. contactors. They have proposed $ND/\sqrt{(T)}$ as the scale-up parameter. Juvekar[48] has used data of Mehta and Sharma[47] and his own data from 0.75 and 1.0 m i.d. contactors to arrive at a rational criteria. It appears that, above the critical impeller speed, V_G has no effect on a and k_La if disk turbine is used as the impeller. Several correlating parameters such as:

$$\frac{ND}{\sqrt{T}}, \frac{(N-N_0)D}{\sqrt{T}}, \left(\frac{P_G}{V}\right)^{0.4} \text{and} \left(\frac{P_G}{V}\right)^{0.6} \epsilon_G^{0.5}$$

were used. The values of standard deviation in these cases were 20.1, 21.7, 20.9 and 24.8 percent, respectively. It can be shown that $ND/\sqrt{(T)}$ varies approximately as $(P/V)^{1/3}$ whereas the fourth correlating parameter varies as $(P_G/V)^{0.6}$ and all the parameters correlate a and k_La data in the same range of standard deviation. Here again it may be emphasized that practically the same gas–liquid system was used in all the cases.

From the foregoing, it can be seen that the development of a generalised correlation covering all the gas–liquid systems appears to be very difficult. There is a need for data on larger size contactors of 1 m and 2 m over a wide range of operating conditions, where the relative contributions of gassing and mechanical agitation should be varied over a broad range.

4.3 *Procedures for scale-up*

Mehta and Sharma[47] and Juvekar[48] have shown that the values of a and k_La vary inversely as the square root of the contactor diameter in the range $0.125 < T < 1$ m. Recently Chandrashekharan and Calderbank[69] have shown that the values of k_La vary approximately as T^{-3} in the range $0.38 < T < 1.22$ m. The experiments in 1.22 m i.d. vessel were performed below the critical impeller speed and the dependence of the contactor diameter, in this case probably needs further examination. Nevertheless it may be recommended that the selection of contactor diameter beyond 1 m should be done with caution and for larger volumes the use of multistage mechanically agitated contactor should be considered.

It is known that the presence of small amounts of surface active agents and electrolytes can markedly change the values of a and k_La. Further the selection of the scale-up parameter has been very difficult. The following procedure should be adopted.

The values of a and k_La vary as $(P_G/V)^{0.25-0.65}$ whereas the operating cost of the power varies linearly

Table 6. Details of range of variables and systems used for heat transfer in presence of gas

Sr. No.	Reference	System used	T and H m vessel Diameter and Height	D m Impeller details	Coil/ Jacket	Range of variables
1.	Zlokarnik [81]	air–sodium sulphite solution	0.4 H = T	0.133 Triangular gas Inducing type	Coil	N_{ReGT} = 1680 to 10,000, N_{Ren} = 1×10^5 to 6×10^5 N_{FrT} = 7.2×10^{-7} to 1.6×10^{-4} v_G = 0.0042 to 0.025 N = 500 to 1500 rpm
2.	Rao and Murthi [71]	air–water air–transformer oil Downward discharge ring sparger	0.70 0.226 H_L = 0.89 H_L = 0.226	0.233 0.075 Turbine impeller H_a = D	Coil and jacket	N = 40 to 500 rpm, v_G = 0.002 to 0.083 $\frac{m}{sec}$ Nu = 700–5000, N_{Re_n} = 1×10^3 to 5×10^5 N_{Pr} = 2–266, N_{Fr} = 0.008 to 0.53 $\frac{\mu_w}{\mu}$ = 0.18–0.98, $\frac{\mu_c}{\mu}$ = 1.02–1.50
3.	Maeteleire [72]	air–water Porous sintered plate sparger	T = 0.180 H_L = 0.204 m	0.10 m	Coil	N = 100–800 rpm, v_G = 0.1976–1.5814 $\frac{m}{sec}$ Nu = 182–1555, N_{Re_n} = 169–261000 N_{Pr} = 2.97–1270, N_{Vi} = 0.243–0.904 N_{We} = 35–6263, N_{Fr} = 0.027–2.009
4.	Steiff and Weinspach [74]	air–water sintered plate spread across reactor cross section	T = 0.19 m = 0.45 m = 0.70 m $1 \le \frac{H}{T} \le 3$	Turbine impeller	Coil	N_{Ren} = 0 to 2.2×10^5, N_{ReG} = 0.5–16000 N_{FrG} = 1.6×10^{-9} to 4×10^{-2} N_{Pr} = 4 to 825

with P_G. Therefore, the selection of the volume of the vessel should probably be based on the minimum total cost. We should start, with a small scale apparatus (say 30 to 40 l) using a fully baffled standard disk turbine. Experiments should be performed with the specified system. The initial concentration of the liquid phase reactant, and the partial pressure of the solute gas and the temperature are selected at the levels which will be representative of the commercial operation. The experiments in the laboratory may be performed in a semi-batch manner but if the dispersion characteristics change as a function of time then continuous experiments are desired. Alternately if the batch-times are small it would be necessary to go for CSTR. The levels of conversion with respect to the liquid phase reactant and the solute gas are decided in advance. It may be noted that the outlet partial pressure of the solute gas increases with time in the semi-batch mode of operation (Juvekar and Sharma [70]). The impeller speed is selected for a value of P_G/V. The volumetric flow rate of gas is adjusted so as to get the solute gas conversion at the predetermined range. A plot of conversion with respect to the liquid phase reactant versus time is obtained. The procedure is repeated at 3–5 values of P_G/V in the range 0.2–10 kW/m^3. If the overall rate of reaction does not increase with an increase in the impeller speed or levels off at certain impeller speed (N^*) then the overall operation is kinetically controlled and the impeller speed can well be selected below N^*. If the rate of heat transfer is rate limiting step then the impeller speed need be selected on the basis of reasonable heat transfer rate.

For the purpose of scale-up Mehta and Sharma [46] have proposed that a and k_La vary as ($NDT^{1/2}$) and this correlation is recommended. The recent work of Lopes de Figueiredo and Calderbank [68] also supports the above relationship. The values of a and k_La decrease with a decrease in P_G/V and the contactor volume will increase for predetermined values of batch time or capacity. From the knowledge of laboratory scale experiments the relationship between the vessel volume and the power consumption can be established for a given batch time or capacity. For this purpose the knowledge of the degree of mixing as a function of the scale of operation is necessary. It is shown that when the mixing time is very small as compared with the reaction time then the liquid phase can be assumed to be completely mixed. This condition is most likely satisfied in the case of gas-liquid reactions for which the mechanically agitated contactors are employed. As regards to the gas phase backmixing very little information is available and for conservative estimations it may be assumed that the gas phase is also completely backmixed.

For the semi-batch operation the batch time is obtained at various P_G/V and for a given level of conversion from the small scale apparatus. If the commercial operation is continuous then the rate at the corresponding liquid phase concentration is obtained from the small scale equipment. In this case also the optimum selection of the contactor volume and the power consumption can be achieved.

It can be seen that a compromise is necessary between P_G/V and contactor volumes. From this relationship the vessel volume is selected for which the total [fixed and the operating (power consumption)] cost is minimum.

5. HEAT TRANSFER

There are several industrially important reactions, such as, oxidation, hydrogenation, halogenation, etc, which are accompanied by large heat effects. For maintaining the desired temperature the heat is removed either through the vessel wall or through a coil or tube bundle immersed in the liquid. A knowledge of heat transfer coefficients for the different heat transfer elements is necessary for a rational design.

Rao and Murthy[71] have studied heat transfer in 0.226 m and 0.7 m i.d. mechanically agitated contactors using flat blade turbine. The details are given in Table 6. They have suggested the following dimensionless correlations:

Jacket

$$\frac{h_j T}{k} = 1.35(N_{Re}^{*})^{0.59}(N_{Pr})^{0.33}\left(\frac{\mu_{wall}}{\mu_{bulk}}\right)^{-0.14}(N_{Fr})^{-0.10} \tag{30}$$

Coil

$$\frac{h_c T}{k} = 0.87(N_{Re}^{*})^{0.64}(N_{Pr})^{0.33}\left(\frac{\mu_{wall}}{\mu_{bulk}}\right)^{-0.14}(N_{Fr})^{-0.10} \tag{31}$$

where

$$N_{Re}^{*} = \frac{D}{\mu_i}(DN + 4V_G)\rho_L$$

$$N_{Pr} = \frac{\mu_i C_p}{k}, \quad N_{Fr} = \frac{N^2 D}{g}. \tag{32}$$

Maerteleire[72] has obtained data from a 0.18 m i.d. mechanically agitated vessel having pitched blade turbine as an agitator.

The exponent on N_{Re} obtained by Maerteleire[72] (pitched blade turbine) matches well with that of Rao *et al.*[71] (flat blade turbine) which indicates that the type of impeller has very little or no effect on the value of the exponent on N_{Re}.

Pollard and Topiwala[73] have performed experiments in a 300 l fermentor. They have proposed a possible form of a correlation.

Steiff and Weinspach[74] have studied heat transfer in stirred and non-stirred G/L contactors and have proposed a correlation which reduces to the case of bubble columns when N is equal to zero.

Discussion

There appears to be some apparent controversy as regards the effect of the presence of gas on heat transfer coefficient (h.t.c). Rao *et al.*[71] and Maerteleire[72] have concluded that the sparging of gas into an agitated liquid improves the heat transfer coefficient at any impeller speed. By contrast Steiff and Weinspach[74] have observed an increase as well as decrease depending upon the impeller speed.

Rao and Murthy[71] have explained the increase in heat transfer coefficient on the basis of the production of secondary circulatory currents due to the bubble motion. It was found that larger the primary turbulence (higher impeller speed) smaller is the effect of gas sparging and vice-versa. This suggests the existence of a critical impeller speed beyond which gas sparging does not improve the heat transfer coefficient. Rao and Murthy[71] did not study this critical impeller speed and hence they have observed only the increase in the heat transfer coefficients in all the experiments. From the correlation proposed by Westerterp *et al.*[44] the critical impeller speed for the geometry of Rao *et al.*[71] works out to be 13.33 r/s while they had selected 8.33 r/s as the upper limit.

Maerteliere[72] has studied the critical impeller speed which is also the speed needed for complete gas dispersion. He calculated this critical impeller speed using Westerterp's[44] correlation. He found no decrease in heat transfer coefficient even beyond the critical impeller speed, but the rate of increase of heat transfer coefficient with gas sparging rate reduced at higher impeller speed. At some impeller speed the gas sparging did not show any effect on heat transfer coefficient and it remained practically constant.

Steiff and Weinspach[74] have found the existence of critical impeller speed (In their case it works out to be 12 r/s by the procedure reported by Westerterp *et al.*[44]). Below the critical impeller speed gas sparging increased the heat transfer coefficient at all the impeller speeds, but the rate of increase of heat transfer coefficient as a function of gas sparging rate decreased at higher impeller speeds. Further, above the critical impeller speed, at a fixed impeller speed, gas sparging decreased the heat transfer coefficient upto a certain limit of gas sparging rate and then showed no further effect of gas sparging. The decrease in heat transfer coefficient may be due to the reduction in the circulation velocity of liquid due to the reduction in the power consumption.

From the foregoing it can be seen that much more experimental work and a rational theoretical approach is necessary for elucidating the effect of the presence of gas on the heat transfer coefficient. The maximum effect of gas sparging on the heat transfer coefficient is to the extent of 25–30% hence is not an item for serious concern.

6. MULTISTAGE CONTACTORS

The single stage mechanically agitated contactor suffers from the drawback of substantial liquid and gas phase backmixing. Further, with an increase in the vessel diameter, the power input is ineffective in the wall region and the gas dispersion becomes poor. These limitations can be greatly reduced by using multiple impellers and height to diameter ratios greater than one. In addition these multistage units need thinner wall as compared to the single stage units for the same contactor volume and thus can be advantageously used for high pressure operations. A typical multistage contactor is shown in Fig. 8. The ratio of the height of each compartment (H_s) to the column diameter varies in the range of 0.5 to 1.5. The compartments are usually separated by radial baffles in order to reduce the extent of gas and liquid phase backmixing.

6.1 *Power consumption*

Limited information is available in the published literature regarding power consumption in multiple impellers. Bates *et al.*[75] have reported that, nearly five diameters of space between the two consecutive pro-

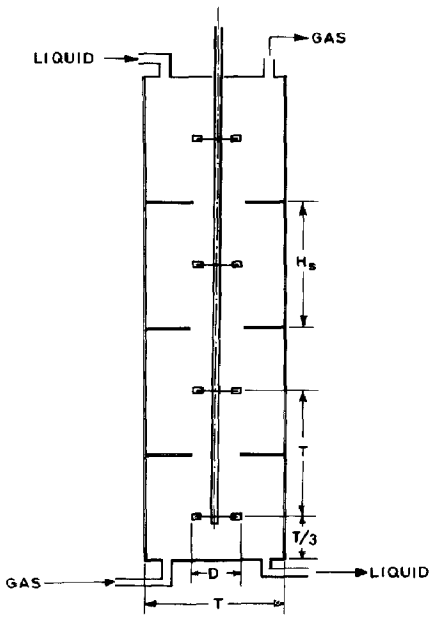

Fig. 8. Multistage mechanically agitated contactor.

pellers is required to consume power equal to twice that consumed by a single propeller. When the spacing is only one impeller diameter the power consumption of two impellers is only about 1.4 times that of the single impeller. By contrast Nienow[76] have reported that the power consumption of two impellers (six bladed disk turbine) is twice that of the single impeller when the spacing is only one impeller diameter. In the presence of gas Nienow *et al.*[76] have reported that the reduction in power consumption is more in the case of single impeller as compared to that when two impellers are employed. This may be due to the fast dispersing action of the lower impeller, dut to which the population of the gas bubbles near the second impeller is not the same. Hence the second impeller is affected to a lesser extent than the first impeller and the reduction in power consumption is not the same as in the case of individual impeller considered alone.

6.2 *Mixing*

Sullivan and Treybal[77] and Haug[78] have reported data on liquid phase axial mixing from 0.15 to 1.5 m i.d. multistage mechanically agitated contactors which were operated in the absence of gas. Sullivan and Treybal[77] have suggested the following correlation for the liquid phase axial dispersion coefficient for 0.15 m i.d. and 12 stages column.

$$\frac{D_L}{H \cdot V_L} = 0.239 + 0.1405 \frac{ND}{V_L}. \tag{33}$$

Recently Joshi[39] has analysed all the reported data on the liquid phase axial mixing from multistage mechanically agitated contactors on the basis of liquid circulation generated by an impeller (disk turbine). The following equation has been proposed:

$$D_L = \frac{0.125 \cdot T \cdot V_c}{n_s} \tag{34}$$

where V_c is the liquid circulation velocity at the column wall (Eq. 2) and n_s is the number of stages in the contactor.

In the presence of gas, Sullivan and Treybal[77] have shown that the extent of liquid phase axial mixing increased with an increase in the superficial gas velocity. The following correlation was suggested:

$$\frac{D_L}{DNH_s} = 227.6\left(\frac{D^2 N \rho_L \epsilon_L^2}{\mu_L}\right)^{-0.928} \tag{35}$$

where

$$\epsilon_L = 1 - \epsilon_G \tag{36}$$

and for

$$N = 0 - 8.33 \text{ r/s}$$

$$\epsilon_G = 6.876 \times 10^{-4} N + 1.874 V_G + 2.31 V_L + 0.052 \tag{37}$$

for

$$N = 8.33 - 33.33 \text{ r/s}$$

$$\epsilon_G = 2.315 \times 10^{-2} N^{0.7} + 0.691 V_G^{0.3} + 0.137 V_L^{0.2} - 0.234. \tag{38}$$

Paca *et al.*[79] have measured mixing time in a 0.51 m i.d. multistage contactor using three impellers. Non-Newtonial fluids with apparent viscosity range 0.001–0.05 Pa.s were employed. In this case also, the mixing time was found to decrease with an increase in the superficial gas velocity.

Gas phase

The only study available on the gas phase axial backmixing is that by Sullivan and Treybal[77]. They could not make quantitative measurements because of the difficulties in sampling and interpretation of data. Through it is expected that the extent of gas phase axial mixing will reduce with an increase in the number of stages, experimental investigations are needed to study the effect of impeller speed, impeller diameter, vessel diameter, number of stages, superficial gas valocity and the physical properties of gas–liquid system, on the gas phase axial dispersion coefficient.

6.3 *Mass transfer*

Juvekar[48] and Ramnarayanan and Sharma[80] have investigated mass transfer characteristics in a 0.2 m i.d. multistage contactors. The interstage baffles were not used and the D/T ratio was maintained at 0.5. The

chemical methods were employed for the measurement of effective interfacial area ($\underline{a}$) and liquid side mass transfer coefficient ($k_L\underline{a}$). It was found that the values of $\underline{a}$ and $k_L\underline{a}$ were independent of the superficial gas velocity. An important conclusion of this study is that the values of $\underline{a}$ and $k_l\underline{a}$ were independent of the number of stages under otherwise identical conditions (D/T ratio, N, V_G, and gas–liquid system). This implies that for the design of multistage reactors, experiments on a single stage contactor should be sufficient as far as mass transfer is concerned. However, studies from larger scale apparatus (say 0.40–0.60 m i.d.) are desirable in order to confirm the above conclusion.

6.4 *Recommendation*

The power consumption of multiple impellers can be calculated assuming that there is no interaction between the impellers. For the estimation of mixing time eqn. (34) is recommended. For the estimation of the effective interfacial area and liquid side mass transfer coefficient, the values of $\underline{a}$ and $k_L\underline{a}$ may be taken same as that provided by single stage units under otherwise uniform conditions.

7. GAS INDUCING TYPE OF AGITATED CONTACTORS

There are several industrially important unit processes, such as hydrogenation, alkylation, ozonolysis, oxidation with molecular oxygen, hydrogenation, ammonolysis, addition halogenation, etc. where it is desirable to have complete utilization of the solute gas. However, the gas phase conversion per pass in a large number of gas–liquid reactions is low in the case of conventional mechanically agitated contactors due to the limited residence time of the gas and/or the low rate of chemical reaction. The external recycle of the gas can be eliminated either by surface aeration or by using self inducing impellers. Gas inducing type of agitated contactors are very popular in flotation, hydrometallurgy operations and in biological waste water treatment.

Many designs of the self inducing impellers are reported in the published literature. Figure 9(a)–(d) shows some of the designs. Zlokarnik[81] had suggested the design as given in Fig. 9(a) with a hollow shaft and a hollow impeller. The impeller consists of a hollow tube which, at the centre, is connected to a hollow shaft. At the two ends of the impeller, cuts at 45° are taken so that, while the impeller is rotating, the open portions are kept at the rear side. Joshi[82] has modified the pipe impeller design. Holes were drilled near the tip of the impeller and on the hub (Fig. 9b). The increase in the liquid flow increases the rate of gas induction by 30–60% at practically the same power consumption.

Martin[83] has used a flattened cylindrical tube so as to simulate the aerofil design (Fig. 9c). In floatation applications, Denver and Wemco type of self inducing impellers are widely used for several decades. Zundelevich[84] has modified the Denver design so as to increase the rate of gas induction by about 100% (Fig. 9d).

7.1 *Critical impeller speed for onset of gas induction*

As a first step in the design of gas-inducing type of agitated contactors it is desirable to know *a priori* the minimum (or critical) impeller speed at which the onset of gas induction occurs. When the impeller is at rest, the value of static pressure at any point on the impeller equals the static head of liquid above it plus the pressure in the gas space. When the impeller is rotating, Bernoulli's equation holds at the surface of the impeller. For an ideal frictionless fluid:

$$d\left(\frac{\rho v^2}{2}\right) + d(p) = 0. \tag{39}$$

The onset of induction will occur when the static pressure at the point of gas induction equals the static pressure in the gas space. Joshi and Sharma[85] have measured the critical impeller speed for pipe and flattened cylindrical impellers and the following correlation has been proposed:

$$\frac{N_{cr}^2 D^2}{gH_L} = \frac{-2}{\pi^2 K}. \tag{40}$$

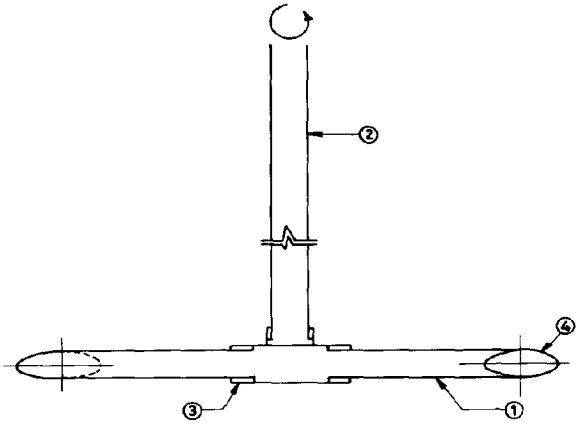

Fig. 9(a). Gas inducing type pipe impeller.

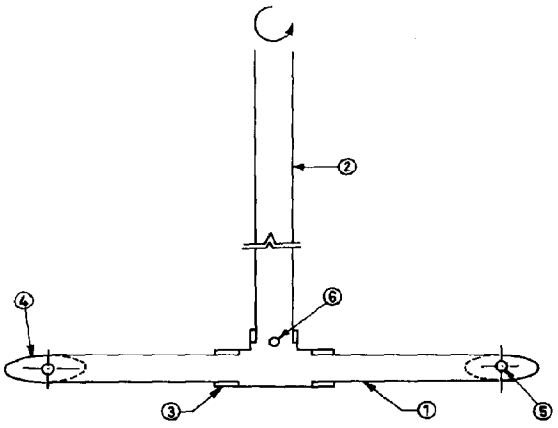

Fig. 9(b). Gas inducing type modified pipe impeller.

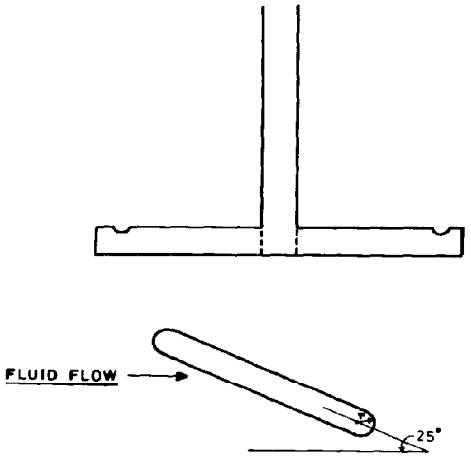

Fig. 9(c). Gas inducing type flattened cylindrical impeller.

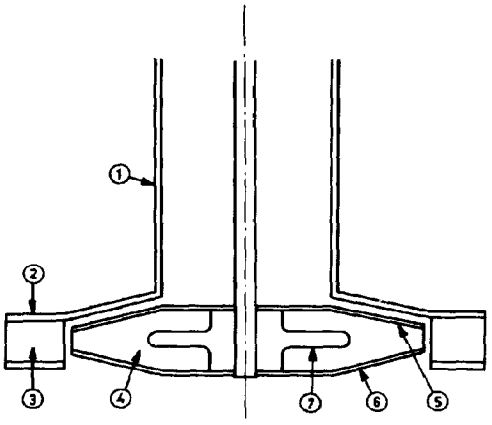

Fig. 9(d). Turbo aerator.

The value of K lies in the range of -0.9 to -1.3.

Sawant and Joshi[86] have measured critical impeller speeds for the Denver and Wemco type of flotation cell. Data on N_{cr} reported by Zlokarnik[81], Martin[83] and White and de Villiers[87] were also analysed. In addition the effect of liquid viscosity has studied in the range of 1 to 80×10^{-3} PaS. The following equation holds within 20 percent:

$$\frac{N_{cr}^2 D^2}{g H_L} \left(\frac{\mu_w}{\mu}\right)^{0.11} = 0.21. \tag{41}$$

7.2 *Rate of gas induction*

When the impeller speed is increased above the critical impeller speed, a pressure driving force is developed, for the gas induction. The rate of gas induction depends upon the impeller design, the impeller speed, the liquid height above the impeller, the physical properties of the liquid and the vessel intervals. Figure 10 shows the rates of gas induction provided by the various impeller designs. In all the cases the liquid volume was about 0.05 m^3, the liquid height 0.4 m and air–water system was employed. It can be seen from Fig. 10 that the modified pipe impeller and the Turbo Aerator provide comparable rates of gas induction. It is likely that the performance of the impellers shown in Fig. 10 is not for optimum designs. When the impeller speed is greater than the critical impeller speed the pressure driving force can be calculated from eqn (40). However, in the presence of gas induction, the density of the dispersion is much lower than the liquid and the actual pressure driving force is substantially lower than that calculated from eqn (40). The theoretical analysis and the prediction of the rate of gas induction is somewhat difficult.

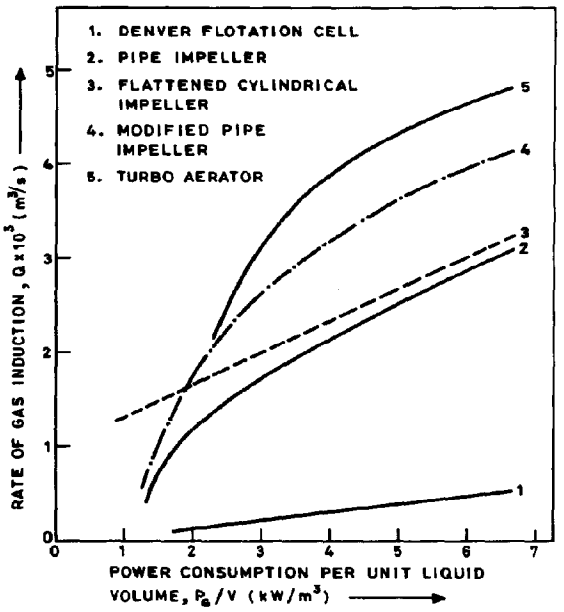

Fig. 10. Comparison of various gas inducing type impellers.

Zlokarnik[81], Zundelevich[84] and Sawant *et al.*[86] have given procedures for the calculation of the rates of gas induction by pipe, Denver and Turbo impellers, respectively.

7.3 *Effective interfacial area and liquid side mass transfer coefficient*

Joshi and Sharma[85] have measured effective interfacial area ($\underline{a}$) and liquid side mass transfer coefficient ($k_L\underline{a}$) in 0.41, 0.57 and 1.0 m i.d. gas induction type of agitated contactors using pipe and flattened cylindrical impellers. For this purpose chemical methods were used and the following correlations have been proposed in the range of ($0.41 < T < 1.0$, $0.35 < D/T < 0.75$, $H_B/T < 0.5$, $0.1 < B < 0.3$ D, $3 < N < 11.7$, $0.3 < V_G < 32$ mm/s)

$$\underline{a} = 112(P_G/V)^{0.4} V_G^{0.5} \quad \text{for} \quad V_G < 5 \text{ mm/s} \tag{42}$$

$$\underline{a} = 36.7(P_G/V)^{0.4} V_G^{0.25} \quad \text{for} \quad V_G > 5 \text{ mm/s} \tag{43}$$

$$k_L\underline{a} = 6.8 \times 10^{-3}(P_G/V)^{0.55} V_G^{0.5} \quad \text{for} \quad V_G < 5 \text{ mm/s} \tag{44}$$

$$k_L\underline{a} = 3.26 \times 10^{-3}(P_G/V)^{0.55} V_G^{0.25} \quad \text{for} \quad V_G > 5 \text{ mm/s}. \tag{45}$$

Joshi and Sharma[85] have shown that, at the same values of power consumption per unit liquid volume, pipe, flattened cylindrical and the disk turbine provide comparable values of $\underline{a}$ and $k_L\underline{a}$. Further, Sawant *et al.*[88,89] have shown that the Denver and the Wemco type of flotation cells also provide comparable values of $\underline{a}$ and $k_L\underline{a}$ to those of pipe and flattened cylindrical impellers at the same value of P_G/V.

7.4 *Heat transfer*

Zlokarnik[81] has studied heat transfer in a 0.4 m i.d. mechanically agitated contactor using triangular hollow gas inducing type of stirrer. He suggested the following correlation for a coil heated fluid:

$$N_{Nu} = 0.185(N_{Re_GT})^{0.733}(N_{Fr_GT})^{-0.267}(N_{PrF})^{0.466} \tag{46}$$

where

$$N_{Re_GT} = \frac{\rho_L v_{G0} T}{\mu_L}$$

$$N_{Fr_GT} = \frac{v_{G0}^2}{gT}$$

and

$$N_{PrF} = \frac{\mu_L C_p}{k_L}.$$

7.5 *Recommendations*

The critical impeller speed N_{cr} for the onset of gas induction may be calculated from eqn (41). For the optimum rate of gas induction the procedure suggested by Zundelevich[84] is recommended. Further experimental investigations for the suspension of solid particles, mixing and heat transfer are needed and newer designs of impellers should be investigated.

8. SURFACE AERATORS

Surface aeration, similar to the case of gas inducing type of agitated contactors, finds important applications for the dead-end systems. Here the gas is introduced above the liquid surface and the gas is entrained into the liquid by the impeller action. In surface aerators there are no compression costs to overcome the static head of the liquid. Surface aerators are extensively used for the waste-water treatment.

8.1 *Minimum impeller speed for surface aeration*

In surface aerators, bubbles are generated at the surface because of the turbulence in liquid phase. These bubbles are entrained into the bulk by the liquid flow generated by the impeller. As a first step in the design of surface aerators it is desirable to know *a priori*, the minimum impeller speed required for the surface aeration. Van Dierendonck *et al.*[90] have proposed the following correlation in the absence of gas sparging:

$$\frac{N_s D}{\left(\frac{\sigma g}{\rho_L}\right)^{1/4}} = 1.55\frac{T}{D}\left(\frac{H - H_l}{T}\right)^{1/2}, \quad V_G = 0 \tag{47}$$

Surface aeration can also occur in the presence of sparging. Calderbank[91] has measured the rate of surface aeration (in the presence of sparging), using six bladed disc turbines ($W/D = 0.2$, $l/D = 0.25$) in 0.3, 0.375 and 0.5 m i.d. mechanically agitated contactors. He has suggested the following correlation:

$$\left(\frac{N_s D^2 \rho}{\mu}\right)^{0.7}\left(\frac{N_s D}{V_G}\right)^{0.3} = 15000. \tag{48}$$

The values of N_s can perhaps be predicted on the basis of liquid flow generated by the impeller. For six bladed disc turbine (h/T*0.5, $l/D = 0.25$) the liquid circulation velocity near the column wall is given by eqn (2)

$$v_{rw} = 0.53\left(\frac{D}{W}\right)ND\left(\frac{D}{T}\right)^{7/6}. \tag{2}$$

The average liquid circulation velocity (V_c) in the bulk can be approximately taken as v_{rw}. The surface aeration will occur when the downward liquid velocity exceeds the terminal rise velocity of bubbles. The average bubble diameter and the terminal rise velocity are given by Bhavaraju *et al.*[92] and Van Krevelen *et al.*[93], respectively:

$$d_B = 1.21\frac{\sigma 0.6}{(P/V)^{0.4}(\rho_L)^{0.2}} \cdot \left(\frac{\mu_L}{\mu_G}\right)^{0.1} \tag{49}$$

$$V_{b\infty} = 0.71\sqrt{(g d_B)}. \tag{50}$$

The surface aeration perhaps starts when V_c equals $V_{b\infty}$. Simplification of eqns (2), (49) and (50) for standard six bladed disk turbine gives:

$$\frac{N_s D^{1.98}}{T^{1.1}} = \frac{1.65}{N_p^{0.125}}\left(\frac{\sigma g}{\rho_L}\right)^{0.19}\left(\frac{\mu_L}{\mu_G}\right)^{0.031}\left(\frac{W}{D}\right)^{0.625} \tag{51}$$

Equation (51) gives the value of N_s as a function of power number, W/D ratio, the characteristic bubble rise velocity ($\sigma g/\rho_L$), the impeller and tank diameters. Figure 11 shows the comparison between the predicted (eqn 51) and the experimental values of N_s.

For the case of air–water system, with W/D of 0.2 and N_p of 5, equation (51) takes the following form:

$$\frac{N_s D^{1.98}}{T^{1.1}} = 1.34\left(\frac{\sigma g}{\rho_L}\right)^{0.19}. \tag{52}$$

Calderbank[91] has reported the values of N_s in the presence of gas sparging. The average liquid circulation velocity is perhaps lower in the presence of gas. It was discussed in Section 2.2 that a reduction in power consumption occurs in the presence of sparging. It is known that the energy supplied by the impeller is used for creating turbulence in the impeller region and for generating the liquid flow. If it is assumed that the fraction of energy dissipated for generating liquid flow remains constant even in the presence of spraging then it can be shown that the average liquid circulation velocity reduces by about 30%, when compared with eqn (2). This reduction was used in predicting N_s in the presence of sparging. From Fig. 11, it can be seen that the agreement between the predicted and experimental values of N_s is reasonably good.

8.2 *Rate of gas entrainment and power consumption*

Any impeller which is capable of generating axially downward flow will create surface aeration. The extent of gas entrainment depends on the turbulence at the liquid surface and the downward volumetric flow rate. Therefore, the impeller design, diameter and its location are very important. Unfortunately a systematic study to investigate the comparative performance of the several impeller designs is not available in the published literature. Matsumura *et al.*[94] have reported the rate of gas entrainment in a 0.218 m i.d. vessel using a disc turbine. Water, ethylene glycol, benzyl alcohol and ethyl alcohol were used as the liquid phase. The following correlation has been proposed:

$$\frac{\eta}{(1-\eta)^2} = 1.913 \times 10^{-10}\left(\frac{V_G}{ND}\right)^{-2.2}\left(\frac{ND^2}{\mu_L}\right)^{0.1} \cdot \left(\frac{N^2 D^3 \rho_L}{\sigma}\right)^{1.38}\left(\frac{N^2 D}{g}\right)^{0.07}\left(\frac{D}{T}\right)^{6.4} \tag{53}$$

where

$$\eta = Q_E/(Q_E + Q) \tag{54}$$

where Q_E and Q are the volumetric flow rates of entrained and sparged gas, respectively. It can be seen from eqn (53) that Reynolds and Froude numbers have nominal effect whereas the D/T ratio and the superficial sparged gas velocity have substantial influence on the rate of gas entrainment.

Recently Matsumura *et al.*[95] have modified the impeller design. A small propeller rotating at high speed is

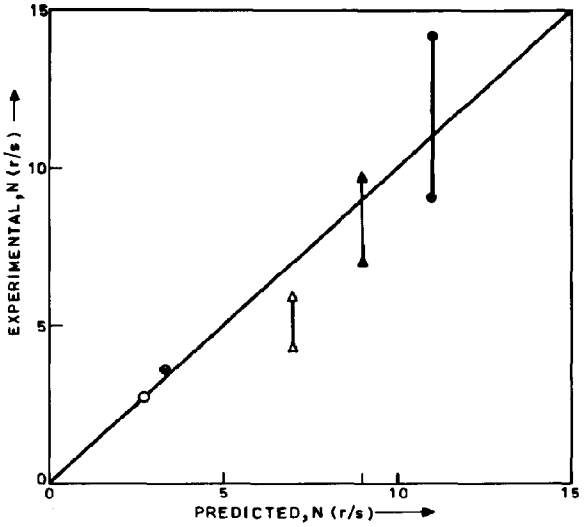

Fig. 11. Comparison between the predicted and experimental values of minimum impeller speed for surface aeration.

Symbol	$T(m)$	$D(m)$	System	Author
○	0.29	0.14	H_2-Aminocapro-lactum solution	[44]
⊗	0.29	0.14	air–water	[44]
△	0.50	0.167	air–water	[8]
▲	0.375	0.125	air–water	[8]
●	0.30	0.10	air–water	[8]

placed near the liquid surface for generating the surface instability and bubbles. The other axial flow turbine is situated at a distance of about one impeller diameter from the bottom. A substantial increase in the rate of gas entrainment has been reported.

Matsumura *et al.*[96] have measured the power consumption in the presence of gas entrainment in the 0.218 m i.d. vessel using a disc turbine impeller. The following correlation has been proposed.

$$\frac{P_G}{P} = 0.26\left(\frac{V_L}{ND}\right)^{-0.2}\left(\frac{N^2D}{g}\right)^{0.055}. \qquad (55)$$

8.3 *Mass Transfer*

Boerma and Lankester[97] have studied the absorption of carbon dioxide in buffer solutions of sodium carbonate and sodium bicarbonate. The results however are not presented in terms of mass transfer parameters. Mehta[98] has obtained the values of effective interfacial area (a) and liquid side mass transfer coefficient (k_La) from 0.125, 0.20, 0.40 and 0.70 m i.d. vessels using six bladed disc turbine as the surface aerator. The values of a and k_La were found to vary in the range of 125 to 325 m^2/m^3 and 0.08 to 0.2 sec^{-1} respectively, when P_G/V was varied in the range of 0.017 to 41.11 kW/m^3.

Teramoto *et al.*[99] have studied the effect of total pressure on the liquid side mass transfer coefficient in a 56 mm i.d. vessel. Unsteady physical absorption of helium and nitrogen was used for the measurement of k_La. The values of k_La were found to be independent of the total pressure.

8.4 *Horizontal agitated contactors*

In the conventional mechanically agitated contactors poor dispersion is likely to occur in large size units particularly near the bottom. This can be overcome by using large L/D ratio with a horizontal arrangement and multiple impellers (Fig. 12). Sasaki[100], Andou *et al.*[101–103] and Joshi and Sharma[104] have investigated the mass transfer characteristics of horizontal agitated contactors. Joshi and Sharma[104] have used 0.38, 0.57 and 1.0 m i.d. horizontal contactors. The values of effective interfacial area and liquid side mass transfer coefficients were obtained by using chemical methods. The optimum liquid submergence ratio (H/T) and the impeller spacing ratio (L_i/D) were found to be in the range of 0.6–0.7 and 1.4–1.6, respectively. The following correlations have been reported:

$$a = 0.3\,NT^{0.6} \qquad (56)$$

$$k_La = 1 \times 10^{-5}N^{1.3}T^{0.6} \qquad (57)$$

where $D/T = 0.5$, $W/T = 1/6$, $H/T = 0.65$, $L_i/D = 1.6$.

8.5 *Recommendations*

For the estimation of minimum impeller speed for surface aeration, eqn (51) is recommended. For the cal-

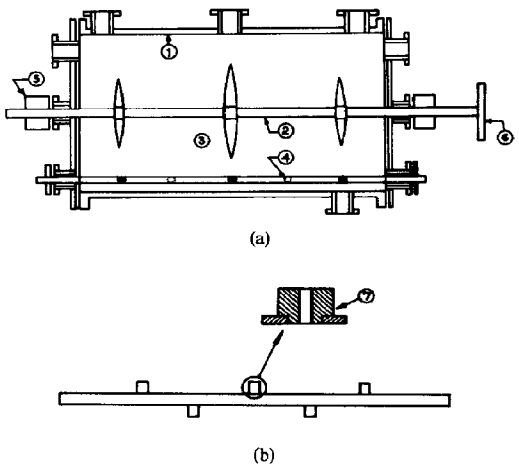

Fig. 12. Horizontal agitated contactor. (1) Horizontal cylindrical vessel. (2) Impeller shaft. (3) Impellers. (4) Nozzle assembly. (5) Gland and stuffiing box. (6) Pulley. (7) Nozzle.

culation of rates of surface aeration, mass transfer coefficients and effective interfacial area, more experimental work, particularly from larger size vessels, is required.

9. NON-NEWTONIAN MATERIALS

In several gas-liquid contacting operations, the liquid phase is non-Newtonian. For example aerobic formentation, biological oxidation of waste water, polymerisation reactions, etc. are conveniently carried out in mechanically agitated contactors. Mashelkar[105] and Doraiswamy and Sharma[106] have reviewed this subject. The rheological complexities of non-Newtonial fluids have been discussed at length in the literature (Astarita and Marrucci[107]).

The dispersion characteristics may be profoundly affected by the fluid behaviour. It is possible that the conventional mass transfer equipment, used for low viscosity Newtonian fluids, may prove to be practically useless for non-Newtonian fluids. Further the scale-up of contactors will pose problems in view of the rheological complexities. In mechanically agitated contactors a non-uniform shear distribution exists. The shear rates will be highest near the tip of the impeller and will decay rapidly as the contactor wall is approached. Thus gas will have a strong tendency to channel through the impeller region in view of the low apparent viscosity in this region and the dispersion characteristics in the contactor will be very poor. Loucades and McManamey[108] have reported the above type of behaviour in the case of fermentation broth which exhibited pseudoplastic behaviour.

In the case of Bingham plastic type of fluids if the yield stress is higher than the characteristic shear stress in the contactor, the gas bubbles may not have any relative motion with respect to the rest of the fluid. In addition to the above factors, the elasticity of fluids may result in a situation, where instead of fluid being thrown away from the impeller, it is sucked in towards the impeller. Viscoelastic liquids reduce the rate of coalescence and also dampen the turbulence. Joshi and Kale[109] have shown that the addition of 50 ppm of polyethylene oxide to aqueous solutions results in about 50% increase in the effective interfacial area and 20% reduction in the liquid side mass transfer coefficient.

The information regarding reduction in power consumption in the presence of gas and the suspension of solid particles in non-Newtonian medium is very scanty in the published literature.

Hocker *et al.*[110] have determined the liquid side mass transfer coefficient using unsteady physical absorption of oxygen. A 0.4 m i.d. vessel was employed and the aqueous solutions of carboxy methyl cellulose and polyacrylamide were used as the liquid phase. They found that the same value of liquid side mass transfer coefficient is obtained as that in the systems having Newtonian liquids at the same value of P_G/V and V_G and is independent of the impeller design. Nishikawa *et al.*[111] have also used the unsteady absorption of oxygen in 0.15, 0.20, 0.30, 0.60 m i.d. vessels to measure k_La. They have reported two correlations for k_La; one for below the critical impeller speed and the other above the critical impeller speed.

For situations where the apparent viscosity is very high, the mechanically agitated contactors cannot be used because of the poor gas phase dispersion. Two types of contactors are commonly used: (i) Mechanically agitated thin film contactor (MATFC) and (ii) Rotating disc contactor (RDC).

Mutzenberg[112] has reported procedures for the calculation of the heat and mass transfer rates in MATFC. Murakami *et al.*[113] have reported some power consumption, hold-up and mass transfer data in RDC. Karandikar and Kale[114] have given a correlation for liquid side mass transfer coefficient in RDC using Newtonian and non-Newtonian liquids:

$$\frac{k_L\delta}{D_A} = 0.063\left\{\frac{\delta(Nd)}{D_A}\right\}^{0.5} \times \left[\frac{N^2d^3\rho}{\sigma}\right]^{0.125} \tag{58}$$

where δ is the liquid film thickness formed over the rotating disk. Data are reported for disks of 125, 175 and 500 mm dia.

9.1 *Heat transfer*

Edney and Edwards[115] have given a correlation to predict heat transfer coefficient in non-Newtonian aerated system. They found no effect of the rate of aeration on heat transfer coefficient.

For 6 bladed turbine:

$$\frac{h_cd_c}{k} = 0.036\left(\frac{ND^2}{\mu}\right)^{0.641}\left(\frac{\mu_AC_p}{k}\right)^{0.353}\left(\frac{D_c}{T}\right)^{-0.375}\left(\frac{\mu_A}{\mu_{Aw}}\right)^{0.2}. \tag{59}$$

The non-Newtonian systems used were carboxy methyl cellulose (0.5–2.0%) and polyacrylamide (0.5–1.5%).

10. DESIGN STRATEGIES AND DIFFERENT MODES OF OPERATION

10.1 *Control of concentration of solute in outgoing gas from semi-batch reactors*

In some cases of industrial importance the solute gas may be obnoxious (for example Cl_2, H_2S, PH_3 etc.) and it becomes necessary to control the concentration of the solute gas in the reactor outlet at a specified value. In some cases for reasons of plant safety the outlet concentration of the solute gas must not be allowed to cross certain threshold value. In a semi-batch reactor, under certain conditions, at the fixed gas flow rate and the composition of the feed gas, the mole fraction of the solute at the outlet increases with time due to the decrease in the concentration of the liquid phase reactant. It is, therefore, necessary to vary with time the feed gas flow rate or the feed gas composition. Alternately the outlet gas composition can be adjusted by adding an inert gas to the outgoing stream deliberately.

10.1.1 *Ideal control strategy.* Here the feed flow rate or the composition is varied continuously in such a way that the mole fraction of the solute in the outlet gas is kept equal to the permissible value, throughout the operation. This can be achieved gy employing a controller in a servo mode in a pre-programmed manner. Juvekar[48] has analysed this problem. The gas and the liquid phases were assumed to be completely backmixed and it was further assumed that the physical properties of the liquid phase did not change during the operation. The case of pseudo first order fast chemical reaction was considered. Under these conditions, the batch time is given by the following equation:

$$t_{B_1} = \frac{2\alpha}{\beta x_0}(\sqrt{([B_0]_i)} - \sqrt{([B_0]_f)}) \tag{60}$$

where

$$\alpha = \frac{V}{z}$$

and

$$\beta = H_c P_{\bar{a}} V_d D_A k_2.$$

It was found that the gas flow rate and the mole fraction of the solute in the feed gas should be varied linearly with time.

10.1.2 *No manipulation of feed gas.* Here the feed gas rate and composition are kept fixed throughout the operation. Their values are adjusted in such a way that at the end of the operation the mole fraction of the solute in the outlet gas reaches the value equal to the threshold limit. For the case of Section 10.1.2 Juvekar[48] has found that the allowable batch time is given by the following equation:

$$t_{B_2} = \frac{\alpha[B_0]_f}{\beta}\left(\frac{\bar{x}_0/x_i}{x_i - \bar{x}_0}\right)\left[\left(1 + \frac{x_i - \bar{x}_0}{\bar{x}_0}\sqrt{\left(\frac{[B_0]_i}{[B_0]_f}\right)}\right)^2 - \left(\frac{x_i}{x_0}\right)^2\right]. \tag{61}$$

This scheme when compared with the ideal control strategy indicates that the value of t_{B_2} is much higher as compared to the batch time when the controller is employed (t_{B_1}). The ratio t_{B_2}/t_{B_1} increases from 1 to 3 when the ratio of final to initial liquid phase concentration ($[B_0]_f/[B_0]_i$) is varied from 1 to 25. When the reactors are expensive the ideal control strategy may be attractive. In other cases the second strategy may be selected because of its simplicity.

10.1.3 *Use of feed-back proportional controller.* Here the inlet gas flow rate is varied proportional to the difference in the outlet composition at any time and at zero time. It is assumed that the lags provided by the measuring element and the control valve are negligible. The value of proportional gain is given by the following equation (Juvekar[48]):

$$k_c = \frac{\beta}{\bar{x}_0 - [x_0]_i}\left[\frac{[x_0]_i\sqrt{([B_0]_i)}}{x_i - [x_0]_i} - \frac{x_0\sqrt{([B_0]_f)}}{x_i - \bar{x}_0}\right]. \tag{62}$$

It can be seen from eqn (62) that the value of k_c depends upon the initial and the final concentrations of the liquid phase reactant and the solute gas. Juvekar[48] has shown that the batch time using proportional controller equals that using the ideal control strategy when k_c is infinite. However, for the overall stability k_c can not be kept at infinity.

10.2 *Gas phase backmixing*

It is known that severe backmixing in the gas phase occurs in mechanically agitated contactors. The extent of backmixing increases with an increase in the impeller speed. If the overall rate of absorption depends upon the partial pressure of the solute gas, then with an increase in the impeller speed the effective driving force decreases (because of backmixing) and the values of mass transfer coefficients ($k_G a$, $k_L a$, $k_{LR} a$) increase. As a consequence, it is likely that an optimum impeller speed exists which gives maximum space time yield (kmole/m^{3}sec). This optimum probably lies in the vicinity of the critical impeller speed given by eqn (27). However, the present day knowledge of the gas phase backmixing is too scanty to select the optimum impeller speed.

10.3 *Mixing and selectivity*

When mixing time is less than one tenth of the average residence time the contents of the vessel can be assumed to be completely backmixed (Van de Vusse[116]). It is well known that chemical reaction rarely occur alone in isolation. A number of side, parallel or consecutive reactions along with the main desired reaction also take place simultaneously. The rate of these reactions decide the overall selectivity. The rates in turn are, however, related to the reactant concentration which vary with the type of flow pattern in the reactor. The selectivity for a specific component can perhaps be obtained by selecting the suitable values of residence time and mixing time.

Bourne *et al.*[117–119] have used fast reactions (fast enough to produce inhomogeneity at the molecular scale) to study the extent of segregation. They developed a diffusion reaction formulation to represent in-

homogeneity in mixtures and its influence on chemical reaction of a mixing dependent product distributions leaving a CSTR. According to the model developed, the product distribution from two competitive, consecutive reactions will be a function of stoichiometric and volumetric ratios of reagents, the ratio of a rate constants, a time parameter and a Thiele-like modulus.

10.4 *Periodic or semi-batch operation.*

Roth *et al.*[120] have shown that the mechanically agitated contactor, when operated in a periodic or semi-batch manner, can produce levels of liquid phase mixing on the macroscale which are intermediate to the limits of plug flow and backmixed operation and which can be selected and controlled to any desired level. Such a scheme is an operational alternative to the tanks in series or plug flow with recycle system, and provides a potential method of increasing the yield of the desired intermediate in complex reaction schemes. Criteria for obtaining desired mixing levels have been reported by Roth *et al.*[120].

10.5 *Shear rate and selection of impeller diameter*

A mechanically agitated contactor contains a variety of sizes, shapes and frequencies of eddies. The resulting maximum size of shear stress elements is determined by the tank and impeller diameters and the impeller speed. There are several examples of shear sensitive processes. The effect of fluid shear stress on the biological solids in fermentation and waste-water treatment, the effect of fluid shear stress on particle size and coagulation in emulsion and suspension polymerisation are examples of shear sensitive processes. There is usually a threshold shear stress below which nothing can happen to shear sensitive processes. It is known that for the same value of P_G/V the shear stress decreases with an increase in the impeller diameter. Further Juvekar[48] has shown that, at the same P_G/V the values of effective interfacial areas and liquid side mass transfer coefficient are independent of D/T ratio. Therefore, it is desirable that, for a particular rate of mass transfer the selection of the impeller diameter and impeller speed should be made in such a way that the level of the shear stress is below the threshold limit.

10.6 *Heat transfer controlled operation*

There are several reactions of industrial importance, such as, chlorination, oxidation etc. which are highly exothermic in nature. It is likely that the overall operation is controlled by the rate of heat removal from the reaction mass and it is considered necessary to maintain the temperature at a desired level. The heat transfer coefficient varies as $(P_G/V)^{0.25-0.33}$ whereas the actual power cost varies linearly with P_G/V. In such cases the problem needs to be analysed for the selection of the optimum volume of the mechanically agitated contactor. When the demand on mass transfer is not important then the radial flow turbine (curved blades) may be used for good rates of heat transfer and this also allows significant saving in power consumption.

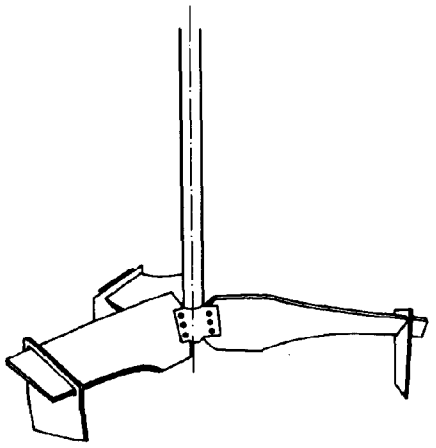

Fig. 13. Modified impeller design (mixing equipment company).

10.7 *Modified impeller design*

Mixing equipment company of U.S.A. have introduced a new impeller design (Fig. 13). It consists of a pitched blade turbine (three blades). At the tip of the impeller, vertical pendant plates are attached. It has been claimed that solids are suspended at a lower value of power consumption as compared to the conventional impellers.

Philadelphia Gear Company has introduced a new design of mechanically agitated contactor. Here the impeller is surrounded by a draft tube. The company has claimed higher values of mass transfer coefficients probably because of the increase in the gas hold-up in the presence of the draft tube. However, the higher values of the gas hold-up will be expected to reduce heat transfer coefficient and the extent of mixing.

10.8 *Single stage vs multistage contactors*

The multistage contactors can be advantageously employed in many situations of practical relevance because of considerably lower extent of backmixing in the gas and liquid phases. For high pressure applications the wall thickness for the multistage contactor is smaller than that for the single stage unit having the same volume. When the vessel diameter is larger than 1 m, it may be very useful to use multistage contactors for the effective utilisation of power (Chandrashekharan and Calderbank[68]). Further, such an arrangement will require less floor space.

11. CONCLUSIONS

(1) The most important parameters which affect the performance of mechanically agitated contactor are the fractional gas hold-up (ϵ_G) and the bubble diameter. At any specified value of power input per unit volume of liquid and V_G the above parameters can have markedly different values and can even vary by an order of magnitude. Even adventitious impurities can affect the above parameters substantially. Thus it is not advisable to

adopt completely generalised correlations and instead it is recommended that the experiments are made with a specified system under the relevant operating conditions in 30–40 *l* capacity reactors and the scale-up is attempted on the basis of correlations reported in this review [Section 2 to 10].

(2) The hydrodynamics of agitated contactors with different types of impellers can be characterised reasonably well in the absence of gas (Section 2.1).

(3) The reduction in power consumption in the presence of gas can be calculated with a fair degree of confidence (Section 2.2).

(4) The presence of gas makes suspension of solid particles more difficult. It is possible to predict the increased power consumption required for complete suspension of solid particles (Section 2.3).

(5) Mixing time with different types of impellers can be calculated in a satisfactory manner on the basis of eqns (14), (18)–(21). The liquid phase is essentially backmixed. The gas phase may be completely backmixed or partially backmixed (Section 2.4).

(6) The use of generalised correlations for calculating $k_L a$ and a involves a large risk and hence procedure suggested in 11.1 should be adopted.

(7) Heat transfer coefficients can be calculated with sufficient engineering accuracy. When demand on mass transfer is not large but heat transfer is more important than curved blade turbines (radial flow) can be advantageously employed due to higher heat transfer coefficient or lower power consumption under otherwise similar conditions. Axial flow turbines and disc turbines are recommended when higher shear rates are desirable. (Sections 4 and 5).

(8) In dead-end type agitated reactor it is beneficial to employ an additional smaller impeller of about 25–30% of the main impeller diameter at a location of liquid surface (rotating at a speed of 2 to 3 times that of larger impeller) for generating surface instability. This greatly enhances the values of the mass transfer coefficient with hardly any increase in the power consumption.

(9) For large capacity contactors the standard designs of mechanically agitated contactors with H/T ratio of 1 to 1.5 are unlikely to be economically attractive due to poor efficiency of the power utilisation. However, multistage contactors with high H/T ratio (of even 6–8) are likely to be attractive from the point of view of wall thickness, backmixing in the liquid and gas phases, power consumption etc. (Section 6).

(10) Gas inducing impellers are likely to be very attractive when pure gas is used, particularly for contactors upto about 150 cm dia and height (Section 7).

(11) Surface aerators can be useful in situations where compression costs of gas are very high and compression of corrosive gasses can also be avoided (Section 8).

(12) In the case of non-Newtonian fluid special attention has to be given to cater for their rheological behaviour (Section 9).

(13) There is a definite need for further work on various important aspects and these are covered in Section 12.

12. RECOMMENDATIONS FOR FURTHER WORK

(1) In the past, most of the experiments have been performed with 0.15–0.4 m i.d. contactors. However, for reliable scale-up it is highly desirable to obtain data from contactors equal to or greater than 1 m diameter. An impressive range of physical properties of liquid should be covered and studies should also be made with different types of non-Newtonian liquids.

(2) (i) Velocity field and the turbulence field (scale and intensity) need to be studied for gas–liquid systems.

(ii) Data on the reduction in power consumption in the presence of gas are needed for liquid having higher viscosities and non-Newtonian behaviour.

(iii) Further work is required for the suspension of particles in gas–liquid contactors to allow a reliable *a priori* prediction, particularly for more viscous materials and asorted particle sizes.

(iv) There are practically no data on the liquid phase mixing time in the presence of gas. The effects of impeller design and diameter, vessel diameter, superficial gas velocity and the physical properties of liquid on mixing time need to be studied.

(v) The backmixing in the gas phase has received scant attention despite its great practical relevance. The effect of solid particles on gas phase backmixing has to be systematically studied.

(vi) Mass transfer data in high pressure reactors operated at higher temperatures and also under refluxing conditions at ambient pressure should be obtained. Initially such studies may be made in a 30–50 cm diameter contactor.

(vii) There are hardly any data on gas-side mass transfer coefficient and hence data should be obtained for single and multistage contactors.

(viii) The reported data on heat transfer coefficient indicate discrepancies as regards the effect of the presence of gas. The range of vessel diameter, impeller diameter should be varied over a wider range. The effect of the physical properties of the liquid, including the non-Newtonian behaviour need to be investigated.

(ix) The multistage contactor are likely to be attractive but data on the various design parameters are scanty. For high pressure applications the optimum L/D ratio is about six (Brownell and Young[121]). The flow patterns, power consumption, mixing and heat transfer in the presence of gas need to be investigated for larger vessels and L/D ratios upto six. The optimum spacing between the impellers should also be studied.

(x) There is scope for improvements in the design of gas inducing impellers. Data on solid suspension, mixing and heat transfer are needed for new impeller designs. In the case of dead-end agitated reactors, a further study is desirable to arrive at optimal parameters for the additional smaller impellers.

(xi) A comparative study on the performance of various designs of the surface aerators is not available in the published literature. Further studies should include this aspect. Data on heat transfer and mixing are also not available.

(xii) It is known that the crystal size is affected in the

case of contact nucleation by the material of construction of an impeller (Shah *et al.*[122]). Such a situation may be of importance in the case of *g/l* contactors when product appears in the form of a precipitate or as crystals. This effect of material of construction (hard or soft) of an impeller needs to be explored further.

NOTATION

A a constant, eqn (27)
a effective interfacial area, m^2/m^3
B a constant, eqn (27)
$[B]$ liquid phase concentration, kgmole/m^3
C_p specific heat, J/kg °C
D diameter of the impeller, m
D_c coil helix diameter, m
D_L liquid phase axial dispersion coefficient, m^2/s
D_A diffusivity, m^2/s
d disk diameter, m
d_B average diameter of the bubble, m
d_c diameter of the coil, m
g acceleration due to gravity, m/s^2
H height of clear liquid, m
H_B location of baffles from the bottom, m
H_c Henry's constant, kmole/m^3 kN/m^2
H_i height of the impeller from the bottom of the vessel, m
H_L height of the liquid above the impeller, m
H_s height of each compartment in multistage contactor, m
h_c heat transfer coefficient for oil heating, (J/m^2s °C)
h_j heat transfer coefficient for jacket heating, (J/m^2s °C)
k thermal conductivity, (J/m °Cs)
k_Ga gas side mass transfer coefficient, (kmole/mskN)
k_La liquid side mass transfer coefficient, s^{-1}
k_{LR} liquid side mass transfer coefficient with chemical reaction, s^{-1}
k_2 second order reaction rate constant, m^3/kgmole s
L_i impeller spacing in horizontal agitated contactor, m
n,N impeller speed, r/s
N_c critical impeller speed for solid suspension, r/s
N_0 critical impeller speed above which fractional gas hold-up is independent of V_G, r/s
N^* minimum impeller speed above which increase in speed does not improve the overall rate, r/s
N_{cr} critical impeller speed for the onset of gas induction r/s
N_Q dimensionless pumping capacity coefficient
N_p power number
N_s minimum impeller speed for surface aeration, r/s
n_s number of stages in multistage contactor
N_{Re} impeller Reynold's number, $\rho ND^2/\mu$
N_{ReG} impeller Reynold's number in presence of gas, $V_G\rho D/\mu$
N_{Pr} Prandtl's number, $\mu C_p/k$
N_{FrG} Froude number in presence of gas, V_G^2/gD
N_{We} Weber number, $\rho N^2T^3/\sigma$ or $\rho N^2d^3/\sigma$
N_{Vi} viscosity ratio, μ_w/μ
P,P_0 power consumption of an agitator, kW
P_G power consumption in presence of gas, kW
P_g power consumption of an agitator in presence of gas, W
p pressure, N/m^2
Q_G volumetric gas flow rate, m^3/s
T diameter of vessel, m
t time, s
V,V_L volume of liquid, m^3
V_G,V_{G0} gas superficial velocity, m/s
$V_{b\infty}$ bubble terminal rise velocity, m/s
V_c liquid circulation velocity, m/s
V_d volume of dispersion, m^3
z stoichiometric factor

Greek symbols

δ liquid film thickness, m
ϵ_G gas phase hold-up
μ viscosity, Pa.s
ρ_L density, kg/m^3
σ surface tension, N/m
θ time, s

Subscripts

A apparent average
B batch
G gas
L liquid
S solid

REFERENCES

[1] Sachs J. P. and Rushton J., *Chem. Engng Prog.* 1954 **50**(12) 597.
[2] Uhl V. W. and Gray J. B., *Mixing*, Vol I. Academic Press, New York 1966.
[3] Bertrand J., Coudere J. P. and Angelino H., *Chem. Engng Sci.* 1980 **35** 2157.
[4] Wolf D. and Manning F. S., *Can. J. of Chem. Engng* 1966 **44** 137.
[5] Levins D. M. and Glastonbury J. R., *Trans. Inst. Chem. Engrs* 1972 **50** 32.
[6] Aiba S., *A.I.Ch.E.J.* 1958 **4** 485.
[7] Marr G. R. and Johnson E. F., *A.I.Ch.E.J.* 1963 **9** 383.
[8] Calderbank P. H., *Trans. Inst. Chem. Engrs* 1958 **36** 443.
[9] Van't Reit K. and Smith J. M., *Chem. Engng Sci.* 1973 **28** 1031.
[10] Bruijn W., Van't Reit K. and Smith J. M., *Trans. Inst. Chem. Engrs* 1974 **52** 88.
[11] Van't Reit K, Boom J. M. and Smith J. M., *Trans. Inst. Chem Engrs* 1976 **54** 124.
[12] Loiseau B., Midoux N. and Charpentier J. C., *A.I.Ch.E.J.* 1977 **23** 931.
[13] Hassan I. T. M. and Robinson C. W., *A.I.Ch.E.J.* 1977 **23** 48.
[14] Loung H. T. and Volesky B., *A.I.Ch.E.J.* 1979 **25** 893.
[15] Hughmark G., *Ind. Engng, Chem., Proc. Des. Dev.* 1980 **19** 638.
[16] Michel B. J. and Miller S. A., *A.I.Ch.E.J.* 1962 **8** 262.
[17] Pharamond J. C., Roustan M. and Roques H., *Chem. Engng Sci.* 1975 **30** 907.
[18] Bimbinet J. J., M. S. Thesis, Purduc Univ., Lafayette, Indiana 1959.
[19] Zweitering T. N., *Chem. Engng Sci.* 1958 **8** 244.
[20] Kolar V., *Coll. Czech. Chem. Commun.* 1961 **26** 613.
[21] Nienow A. W., *Chem. Engng Sci.* 1968 **23** 1453.
[22] Baldi G., Conti R. and Alaria E., *Chem. Engng Sci.* 1978 **33** 21.
[23] Narayanan S., Bhatia V. K., Guha D. K. and Rao M. N., *Chem. Engng Sci.* 1969 **24** 223.
[24] Subbarao D. and Taneja V. K., *Third European Conference on Mixing*, April 1979.
[25] Einenkel W. D., *Ger. Chem. Engng* 1980 **3** 118.
[26] Joosten G. E. H., *Trans. Inst. Chem. Engrs* 1977 **55** 220.
[27] Short G. B., Private Communication 1980.
[28] Weildman J. A., Steiff A. and Weinspach P. M., *Ger. Chem. Engng* 1980 **3** 303.
[29] Chapman C. M., Nienow A. W. and Middelton J. C., *Trans. Inst. Chem. Engrs* 1981 **59** 134.
[30] Norwood K. W. and Metzner A. B., *A.I.Ch.E.J.* 1960 **6** 432.
[31] Biggs R. D., *A.I.Ch.E.J.* 1963 **9** 636.
[32] Khang S. J. and Levenspeil O., *Chem. Engng Sci.* 1976 **31** 569.
[33] McManamey W. J., *Trans. Inst. Chem. Engrs* 1980 **58** 271.
[34] Holmes D. B., Voncken R. M. and Decker J. A., *Chem. Engng Sci.* 1964 **20** 264.
[35] Brennan D. J. and Lehrer I. H., *Trans. Inst. Chem. Engrs* 1976 **54** 139.
[36] Rao D. P. and Edwards L. L., *Chem. Engng Sci.* 1973 **28** 1179.
[37] Goldstein A. M., *Chem. Engng Sci.* 1973 **28** 1021.
[38] Sasakura T., Kato Y., Yamamura S. and Ohi N., *Int. J. Chem. Engng* 1980 **20**(2) 251.
[39] Joshi J. B., *Trans. Inst. Chem. Engrs.* 1980 **58** 155.
[40] Prochazka J. and Landau J., *Coll. Czech. Chem. Commun.* 1961 **26** 2961.

[41] Van der Molen K. and Van Mannen H. R. E., *Chem. Engng Sci.*, 1978 **33** 1161.
[42] Davies J. T., *Turbulence Phenomena.* Academic Press, New York, 1972.
[43] Einsele A. and Flnn R. K., *Ind. Engng Chem. Proc. Des. Dev.* 1980 **19** 600.
[44] Westerterp K. R., Van Dierendonck L. L. and De Kraa J. A. *Chem. Engng Sci.* 1963 **18** 157.
[45] Hanhart J., Kramers H. and Westerterp K. R., *Chem. Engng Sci.* 1963 **18** 503.
[46] Gal-Or B. and Resnick W., *Ind. Engng Chem. Proc. Des. Dev.* 1966 **5** 15.
[47] Mehta V.D. and Sharma M. M., *Chem. Engng Sci.* 1971 **26** 461.
[48] Juvekar V. A., Ph.D. (Tech.) Thesis, Univ. Bombay 1976.
[49] Towell G. D., Strand C. P. and Ackerman G. H., *A.I.Ch.E.J. Chem. E. Symp. Ser.* 1965 91.
[50] Burges J. M. and Calderbank P. H., *Chem. Engng Sci.* 1975 **30** 1107.
[51] Schumpe A. and Deckwer W. D., *Chem. Engng Sci.* 1980 **35** 2221.
[52] Calderbank P. H., Evans F. and Rennie J., *Int. Symp. on Distillation*, p. 5. London 1965.
[53] Lokett M. J. and Safekourdi A. A., *A.I.Ch.E.J.* 1977 **23** 395.
[54] Landau J., Gomoa H. G. and Al Taweel A. M., *Trans. Inst. Chem. Engrs* 1977 **55** 212.
[55] Weinstein B. and Treybal R. E., *A.I.Ch.E.J.* 1973 **19** 304.
[56] McLaughlin C. M. and Rushton J. H., *A.I.Ch.E.J.* 1973 **19** 817.
[57] Sharma M. M. and Danckwerts P. V., *Br. Chem. Engng* 1970 **15** 522.
[58] Danckwerts P. V. and Sharma M. M., *Chem. Engr.* 1966 **44** CE244.
[59] Jhaveri A. S. and Sharma M. M., *Chem. Engng Sci.* 1968 **23** 669.
[60] Sridharan K. and Sharma M. M., *Chem. Engng Sci.* 1976 **31** 767.
[61] Midoux N., Laurent A., and Charpentier J. C., *A.I.Ch.E.J.* 1980 **26** 157.
[62] Linek V. and Vacek V., *Chem. Engng Sci.* 1981 **36** 1747.
[63] Van't Reit K., *Ind. Engng Chem. Proc. Des. Dev.* 1979 **18** 357.
[64] Keitel G. and Onken U., *Chem. Engng. Sci.* 1981 **36** 1927.
[65] Sharma M. M. and Mashelkar R. A., *Proc. Symp. on "Mass Transfer with Chemical Reaction"*. The Institution of Chem. Engrs, London 1968.
[66] Juvekar V. A. and Sharma M. M., *Chem. Engng Sci.* 1973 **28** 976.
[67] Miller D. N., *A.I.Ch.E.J.* 1974 **20** 445.
[68] Lopes de Figueiredo M. M. and Calderbank P. H., *Chem. Engng Sci.* 1979 **34** 1333.
[69] Chandrasekhar K. and Calderbank P. H., *Chem. Engng Sci.* 1981 **36** 819.
[70] Juvekar V. A. and Sharma M. M., *Trans. Inst. Chem. Engrs* 1977 **55** 77.
[71] Rao K. B. and Murthy P. S., *Ind. Engng, Chem. Proc. Des. Dev.* 1973 **12** 190.
[72] Maerteleire E. De., *Chem. Engng Sci.* 1978 **33** 1107.
[73] Pollard R. and Topiwala H. H., *Biotech. Bioengng* 1976 **18** 1517.
[74] Steiff A. and Weinspach P. M., *Ger. Chem. Engng* 1978 **1** 150.
[75] Bates R. L., Fondy P. L. and Fenic J. G., *Mixing*, Vol. I, [2]. Academic Press, New York 1966.
[76] Nienow A. W. and Lilly M. D., *Biotech. Bioengng* 1979 **21** 2341.
[77] Sullivan G. A. and Treybal R. E., *Chem. Engng. J.*, 1972 **1** 302.
[78] Haug H. F., *A.I.Ch.E.J.* 1971 **17** 585.
[79] Paca J., Etter P. and Greg V., *J. Appl. Chem. Biotech.* 1976 **26** 309.
[80] Ramnarayanan K. and Sharma M. M., Forwarded for publication 1981.
[81] Zlokarnik M., *Chemie Ing. Technik* 1966 **38** 717.
[82] Joshi J. B., *Chem. Engng Comm.* 1980 **5** 213.
[83] Martin G. Q., *Ind. Engng Chem. Proc. Des. Dev.* 1972 **11** 397.
[84] Zundelevich Y., *A.I.Ch.E.J.* 1979 **25** 763.
[85] Joshi J. B. and Sharma M. M., *Can. J. Chem. Engng* 1977 **55** 683.
[86] Sawant S. B. and Joshi J. B., *Chem. Engng. J.*, 1979 **18** 87.
[87] White D. A. and de Villiers J. U., *Chem. Engng. J.* 1977 **14** 113.
[88] Swant S. B., Joshi J. B. Pangarkar V. G. and Mhaskar R. D., *Chem. Engng J.* 1981 **21** 11.
[89] Sawant S. B., Joshi J. B. and Pangarkar V. G., *Ind. Chem. Engr* 1981 **22** 3.
[90] Van Dierendonck L. L., Fortain J. M. H. and Vanderboss D., *Proc. Fourth European Symp. on Chem. Reaction Engng.* Brussels 1968.
[91] Calderbank P. H., *Trans. Inst. Chem. Engrs* 1959 **37** 173.
[92] Bhavaraju S. M., Russel T. W. F. and Blanch H. W., *A.I.Ch.E.J.* 1978 **24** 454.
[93] Van Krevelen D. W. and Hoftizer P. J., *Chem. Engng Prog.* 1950 **46** 29.
[94] Matsumura M., Masunga H. and Kobayashi J., *J. Ferm. Tech* 1977 **55** 388.
[95] Matsumura M., Sakuma H., Yamagata T. and Kobayashi J., *J. Ferm. Tech.* 1980 **58** 69.
[96] Matsumura M., Masunga H., Haraya K. and Kobayashi J., *J. Ferm. Tech.* 1978 **56** 128.
[97] Boerma H. and Lankester J. H., *Chem. Engng Sci.* 1968 **23** 799.
[98] Mehta V. D., Ph.D. (Tech.) Theses, Univ. Bombay 1970.
[99] Teramoto M., Tai S., Nishi K. and Teranishi H., *Chem. Engng J.* 1974 **8** 223.
[100] Sasaki, E., *Ind. Chem. Japan* 1971 **74** 9.
[101] Andou K., Hara H. and Endoh K., *Kagaku Kogaku* 1971 **35** 1379.
[102] Andou K., Talso H. and Endoh K., *J. Chem. Engng Japan* 1972 **5** 193.
[103] Andou K., Fukuda T., Sato K. and Endoh K., *Kogaku Kogaku* 1974 **38** 540.
[104] Joshi J. B. and Sharma M. M., *Can. J. Chem. Engng* 1976 **54** 560.
[105] Mashelkar R. A., *Chem. Ind. Dev.* 1976 **10** 17.
[106] Doraiswamy L. K. and Sharma M. M., *Heterogeneous Reactions—Analysis, Examples and Reactor Design.*, John Wiley and Sons, New York (1981) in Press.
[107] Astarita G. and Marrucci G., *Principles of non-Newtonian Fluid Mechanics.* McGraw Hill, New York 1974.
[108] Loucades R. and MacManamey W. J., *Chem. Engng Sci.* 1973 **28** 2165.
[109] Joshi J. B. and Kale D. D., *Chem. Engng Commun* 1979 **3** 15.
[110] Hocker H., Langer G. and Werner U., *Ger. Chem. Engng* 1981 **4** 51.
[111] Nishikawa M., Nakamura M. and Hashimoto K., *J. Chem. Engng Japan* 1981 **14** 227.
[112] Mutzenberg A. B., *Chem. Engng* 1965 **72** 175.
[113] Murakami Y., Fujimato K., Kakimoto K. and Sekiho M., *J. Chem. Engng Japan* 1972 **5** 257.
[114] Karandikar B. M. and Kale D. D., Private Communication 1981.
[115] Edney H. G. S. and Edwards M. F., *Trans. Inst. Chem. Engrs.* 1976 **54** 160.
[116] Van de Vusse, J. G., *Chem. Engng. Sci.* 1962 **17** 507.
[117] Bourne J. R., Kozicki F. and Rys P., *Chem. Engng Sci.* 1981 **36** 1643.
[118] Belevi H, Bourne J. R. and Rys P., *Chem. Engng Sci.* 1981 **36** 1649.
[119] Bourne J. R., Kozicki F., Moergelli U. and Rys P., *Chem Engng Sci.* 1981 **36** 1655.
[120] Roth D. D., Basaram V. and Seagrave R. C., *Ind. Engng Chem. Fundls* 1979 **18** 376.
[121] Brownell L. E. and Young E. H., *Process Equipment Design.* Wiley Eastern 1977.

[122] Shah B. C., McCabe W. L. and Rouseau R. W., *A.I.Ch.E.J.* 1973 **19** 194.
[123] Clark M. W. and Vermeulen T., Power requirements for mixing of gas–liquid systems. *UCRL–10996, University of California, Berkeley* 1963.
[124] Yung C. N., Wang C. W. and Chang C. L., *Can. J. Chem. Engng* 1979 **57** 672.
[125] Fox E. A. and Gex V. E., *A.I.Ch.E.J.* 1956, **2**, 539.
[126] Kramers H., Barrs G. M. and Knoll W. H., *Chem. Engng Sci.* 1953 **2** 35.
[127] Van de Vusse, *Chem. Engng Sci.* 1955 **4** 178.
[128] Wesselingh J. A., *Chem. Engng Sci.* 1975 **30** 973.
[129] Mersmann A., Einenkel W. D. and Kappel M., *Int. Chem. Engng* 1976 **16** 590.
[130] Burghardt A. and Lipowska L., *Chem. Engng Sci.* 1972 **27** 1783.
[131] Prasher B. and Wills G. B., *Ind. Engng, Chem. Proc. Des. Dev.* 1973 **12** 351.
[132] Hassan I. T. M. and Robinson C. W., *Chem. Engng Sci.*, 1980 **35** 1277.
[133] Hassan I. T. M. and Robinson C. W., *Can. J. Chem. Engng* 1980 **58** 198.
[134] Sridhar T. and Potter O. E., *Ind. Engng Chem., Fundls* 1980 **19** 21.
[135] *Mannual for Experimental Agitator Model ELB* Chemineer, 1966. Ohio,
[136] Voncken R. M., *B. Chem. Engng* 1965 **10**(1) 12.
[137] Charpentier J. C. and Midoux N., *Entropie* No. 88, 5, 1979.